

INTERIM REPORT

Underwater Munitions Expert System to Predict Mobility and
Burial

SERDP Project MR-2227

AUGUST 2015

Sarah Rennie
Alan Brandt
Johns Hopkins University

Distribution Statement A
This document has been cleared for public release



This report was prepared under contract to the Department of Defense Strategic Environmental Research and Development Program (SERDP). The publication of this report does not indicate endorsement by the Department of Defense, nor should the contents be construed as reflecting the official policy or position of the Department of Defense. Reference herein to any specific commercial product, process, or service by trade name, trademark, manufacturer, or otherwise, does not necessarily constitute or imply its endorsement, recommendation, or favoring by the Department of Defense.

REPORT DOCUMENTATION PAGE

Form Approved
OMB No. 0704-0188

Public reporting burden for this collection of information is estimated to average 1 hour per response, including the time for reviewing instructions, searching existing data sources, gathering and maintaining the data needed, and completing and reviewing this collection of information. Send comments regarding this burden estimate or any other aspect of this collection of information, including suggestions for reducing this burden to Department of Defense, Washington Headquarters Services, Directorate for Information Operations and Reports (0704-0188), 1215 Jefferson Davis Highway, Suite 1204, Arlington, VA 22202-4302. Respondents should be aware that notwithstanding any other provision of law, no person shall be subject to any penalty for failing to comply with a collection of information if it does not display a currently valid OMB control number. **PLEASE DO NOT RETURN YOUR FORM TO THE ABOVE ADDRESS.**

1. REPORT DATE (DD-MM-YYYY) 21-August-2015			2. REPORT TYPE Interim Report		3. DATES COVERED (From - To)	
4. TITLE AND SUBTITLE Underwater Munitions Expert System: Preliminary Design Report			5a. CONTRACT NUMBER W912HQ-12-C-0032		5b. GRANT NUMBER	
			5c. PROGRAM ELEMENT NUMBER		5d. PROJECT NUMBER MR-2227	
			5e. TASK NUMBER		5f. WORK UNIT NUMBER	
6. AUTHOR(S) Sarah E. Rennie Alan Brandt			8. PERFORMING ORGANIZATION REPORT NUMBER			
7. PERFORMING ORGANIZATION NAME(S) AND ADDRESS(ES) Johns Hopkins University Applied Physics Lab 11100 Johns Hopkins Road Laurel, MD 20723			10. SPONSOR/MONITOR'S ACRONYM(S) SERDP			
9. SPONSORING / MONITORING AGENCY NAME(S) AND ADDRESS(ES) Strategic Environmental Research and Development Program (SERDP) 4800 Mark Center Drive Suite 17D08 Alexandria VA 22350-3600			11. SPONSOR/MONITOR'S REPORT NUMBER(S)			
			12. DISTRIBUTION / AVAILABILITY STATEMENT Approved for public release; distribution is unlimited			
13. SUPPLEMENTARY NOTES N/A						
14. ABSTRACT This document describes the rationale for, and preliminary design of a computer-based probabilistic expert system to predict the likelihood of burial and migration of abandoned underwater munitions. The objective of this project is to develop a computer-based probabilistic expert system that synthesizes recent and new research to model munitions burial and mobility in a range of underwater environments. As there are numerous inland water and coastal sites contaminated with UXO, to support planning for efficient site remediation, it is important to have a predictive mechanism for identifying the locations and degree of burial of extant UXO. Key to providing this predictive capability is knowledge of the process and time scales for the scour, burial, re-exposure, migration, and subsequent reburial of UXO resident in the sediments at the sites of interest.						
15. SUBJECT TERMS						
16. SECURITY CLASSIFICATION OF:			17. LIMITATION OF ABSTRACT SAR	18. NUMBER OF PAGES 46	19a. NAME OF RESPONSIBLE PERSON Dr. Sarah Rennie	
a. REPORT U	b. ABSTRACT U	c. THIS PAGE U			19b. TELEPHONE NUMBER (include area code) 443-778-8178	

Underwater Munitions Expert System: Preliminary Design Report

Sarah E. Rennie and Alan Brandt

Johns Hopkins University Applied Physics Laboratory

Table of contents

Summary

1. Introduction

1.1 Scope of the present study

2. Design of UnMES

2.1. Introduction to Bayesian Networks

2.2. Nodes, Links and Conditional Probability Tables

2.3. Spatial Distribution: Replicas of the Bayesian Network

2.4. Temporal Evolution

3. Details of Nodes in UnMES

3.1. Rationale for Discretization: Bottom Velocity Example

3.2. Input Nodes: Geologic Setting

3.2.1. Sediment characterization

3.2.2. Water Depth

3.3. Input Nodes: Wave Forcing

3.3.1. Shallow Water Wave Transformation

3.3.2. Discretization of Wave Height and Period

3.3.3. Wave Direction

3.4. Input Nodes: Distribution of UXO

3.4.1. UXO Type & Abundance

3.4.2. Initial Burial

3.5. Input Nodes: Probability of Erosion or Accretion of Sediments

3.6. Intermediate Nodes: Scour Burial and Total Burial

3.7. Results Nodes: Migration probability

3.7.1. Migration Distance

3.7.2. Migration Direction

4. Core Physics: process models in UnMES

4.1. Scour Burial Model

4.2. Mobility Model

4.3. Re-exposure Models

5. Example Implementation

6. Summary and Future Work

Underwater Munitions Expert System: Preliminary Design Report

Acronyms

API	- Application Programmer Interface
APL	- Applied Physics Laboratory
BN	- Bayesian Network
CERCLA	- Comprehensive Environmental Response, Compensation, and Liability Act
CFD	- Computational Fluid Dynamics
CPT	- Conditional Probability Table(s)
CSM	- Conceptual Site Model
DBDB-V	- Digital Bathymetric Data Base, Variable resolution (DBDBV)
d_{sed}	- Sediment grain size
EPA	- Environmental Protection Agency
ESTCP	- Environmental Security Technology Certification Program
FRF	- Field Research Facility, USACE, Duck, North Carolina
GIS	- Graphical Information System
GoM	- Gulf of Mexico
h_{sigma}	- Standard deviation of bathymetry about the mean (temporal)
JALBTCX	- Joint Airborne Lidar Bathymetry Technical Center of Expertise
JHU	- The Johns Hopkins University
MEC	- Munitions and Explosives of Concern
MR	- Munitions Response
NAVFAC	- Naval Facilities Engineering Command
NAVOCEANO	- Naval Oceanographic Office
NCEP	- National Centers for Environmental Prediction
NRL	- Naval Research Laboratory
NWPS	- Nearshore Wave Prediction System
ONR	- Office of Naval Research
PDF	- Probability Distribution Function
PMF	- Probability Mass Function
QGIS	- Open-source desktop GIS application formerly called Quantum GIS
SERDP	- Strategic Environmental Research and Development Program
STWAVE	- Steady State Spectral Wave Model
SWAN	- Simulating WAves Nearshore, 3 rd generation wave model
U_{bot}	- Velocity of fluid flow at the bottom of the water column
UnMES	- Underwater Munitions Expert System
USACE	- United States Army Corps of Engineers
UXO	- Unexploded Ordnance
WHOI	- Woods Hole Oceanographic Institution

Underwater Munitions Expert System: Preliminary Design Report

S. E. Rennie and A. Brandt JHU/APL

Summary

This document describes the rationale for, and preliminary design of a computer-based probabilistic expert system to predict the likelihood of burial and migration of abandoned underwater munitions.

1. Introduction

As a legacy of years of naval activities, including training and testing, there are numerous current and former Department of Defense (DoD) aquatic sites contaminated with munitions and explosives of concern (MEC). At many of these inland water and coastal areas, the risk of human interaction with unexploded ordnance (UXO) is of grave concern, and efforts have been mandated to manage and clean up these contaminated sites. The Munitions Response program of the Strategic Environmental Research and Development Program (SERDP) is tasked with developing innovative methods to remediate and sustainably administer areas polluted by discarded munitions. Towards this end, SERDP is sponsoring the development of the Underwater Munitions Expert System (UnMES), for predicting the location of munitions and their degree of burial at underwater sites of interest.

Compared to terrestrial sites, underwater environments are more dynamic, with UXO¹ often subject to mobility, burial, and excavation by bottom currents driven by waves and tides. The extent of the search area covered for a region containing underwater UXO is limited using present platform and sensor technology. Therefore it is advantageous to have the ability to predict areas of munitions concentration, exposure and temporal variability, to support planning for efficient site remediation.

The predictive model UnMES is built on a probabilistic Bayesian network whose construct inherently quantifies and tracks the uncertainty of the predictions. This feeds naturally into risk assessment framework needed by site managers for making informed remediation decisions. Toward this end, the Bayesian network in the UnMES is embedded in a Geographic Information System (GIS) framework to interpret and display spatial variation.

¹ The acronym UXO is used to denote MEC of all types and sources.

The choice of a probabilistic approach is appropriate in situations where there is large inherent uncertainty in the predictive models and particularly in the scope and range of values of the governing input parameters. The state of the art of deterministic coastal system models is at present not sufficient to permit the scaling of first-principle physical processes, such as turbulence-forced sediment suspension that occurs at the scale of a breaking wave, up to the larger coastal morphological response which occurs on timescales from months to years or even decades [Hanson *et al.*, 2003]. In the case of modeling UXO-contaminated sites, there is substantial uncertainty in the boundary and forcing conditions: the initial population of the munitions is usually not well-known, and the environment at the site over the time since the deposition may not have been recorded. Therefore, we must rely upon regional climatological distributions and assume most likely scenarios.

The design of UnMES is focused on providing quantitative probabilistic estimates that address the questions site managers need answered. For example, given an estimate of the initial distribution of UXO, one might want to know from which areas within the field the munitions were more likely to migrate, and in what direction, and thus what specific locations they might potentially aggregate. Furthermore, given knowledge of the types of munitions onsite, one might want to know which types are more subject to mobilization. An important prediction concerns how frequently UXO are likely to be buried versus proud on the surface of the seabed, a factor that significantly impacts the performance of sensors used to detect and classify munitions. Answers in the form of probability distributions can provide risk information, and can be used to evaluate remediation alternatives.

1.1 Scope of the present study

The expert system currently under development will be a core component in the larger effort under the SERDP Munitions Response (MR) Program to develop technologies allowing rapid assessment of large-area underwater sites where detection and remediation of munitions is required. For successful implementation, the overall assessment framework will involve multiple components including:

1. Site specific environmental data and historical military archives.
2. UnMES: probabilistic estimate of UXO migration and burial.
3. Detection sensor performance predictions.
4. Risk assessment based on human exposure and removal issues.
5. Decision support tool providing graphical mapping and visualization of UXO distributions and burial state for site remediation managers and planners.

The present effort is specifically on the development of component 2, the UnMES, whose relationship to the larger system is diagrammed in Figure 1.1. The other components will be part of the long-term SERDP/ESTCP program. To demonstrate and verify the operation of UnMES, however, assessments at specific sites will be undertaken, requiring representative site-specific data to be assembled and utilized.

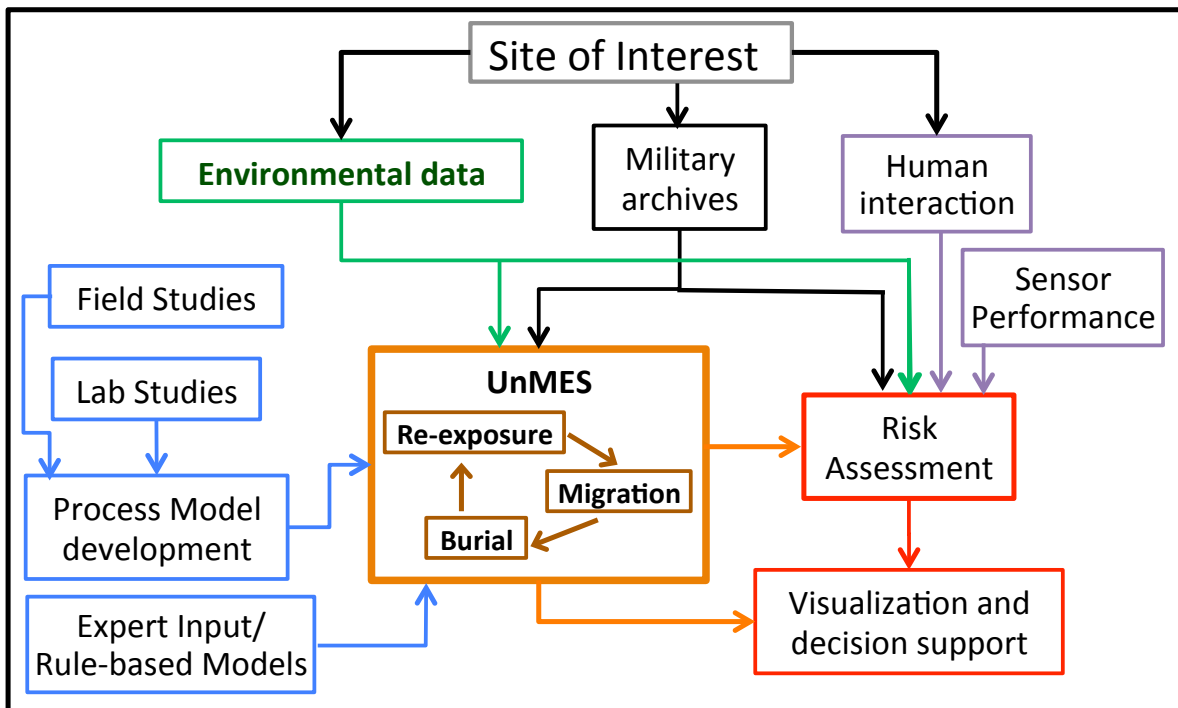


Figure 1.1 Conceptual diagram of components of the SERDP MR program required to characterize risk and plan for remediation efforts at underwater munitions response sites.

The scope of the present effort to develop of the prototype UnMES entails the following tasks:

1. Development of physical and/or data-based process models for mobility, burial, and re-exposure (in collaboration with other SERDP MR studies).
2. Development of a probabilistic BN, including rationale for the discretization of parameter values within the network, and methodologies for generation of the conditional probabilities that provide the basis for UXO state predictions.
3. Incorporation of the Bayesian network into a GIS framework to demonstrate the spatial application of probabilistic prediction.
4. Acquisition of data from representative sites of interest for demonstration and verification purposes using extant databases and current SERDP studies.
5. Demonstration GIS mapping of UXO accumulation and burial probabilities at representative sites.

These development efforts are being supported by modeling, laboratory and field studies under by the SERDP MR program, especially Friedrichs (VIMS) and Garcia (U. Illinois) for Task 1; along with Jenkins (SIO), Traykovski (WHOI), and Calantoni (NRL) for Task 4.

In order to provide useful estimates of munitions behavior probabilities, sufficient environmental data is required for understanding the geologic setting and primary wave and current forcing. The more detailed and extensive the available background environmental data the more accurate and specific the resulting predicted probability distributions will be. However, UnMES is designed to provide estimated probabilities even when the input description is broad or generic.

2 Design of UnMES

The central paradigm of UnMES is a Bayesian Network [Pearl, 1988], a graphical probability model that reflects current knowledge of the likely behavior of UXO migration and burial in a given environment, as illustrated in Figure 2.1. This core construct should be placed in a 2-D map framework in order to accommodate spatially varying input parameters, and to distribute resulting predictions in a map-based management tool. Populating the 2-D framework with the relevant environmental data requires building connections from UnMES to a Geographic Information System (GIS) developed for the site of interest. An overview of this software framework is diagrammed in Figure 2.2. The prototype system now under development will be exercised at sites where input data is currently available. Development of a full-featured management tool where in the UnMES is embedded as a module with GIS support [e.g. Holland, 2014] remains a task for a future phase of the SERDP MR program.

The focus of the preliminary UnMES design will be on wave-dominated climates, where the important environmental forcing is primarily due to the bottom orbital flows from wind-driven waves – a situation of primary interest for remediation efforts; and an environment in which several SERDP field experiments have been conducted and can provide validation data [Calantoni *et al.*, 2015, Traykovski, 2015]. In these regions, encompassing the coastal ocean and large lakes, the sediment is generally comprised of non-cohesive sands. Subsequent to the development and proofing of this prototype version, the design framework can be expanded to include the other underwater environments of interest, including estuaries and rivers, which have different circulation patterns and include additional forcing mechanisms, such as tides, flood erosion and fluvial deposition. Sand sediments under waves are generally resistant to penetration, whereas in estuaries and rivers the bottom type is often soft clays or muds where burial upon initial impact with the

seabed may be important. Additional wave-driven regions with different underlying geology, such as large cobbles, and coral reefs, can be added to future versions of UnMES.

For this preliminary UnMES design, the focus is on seasonal and annual timescales where the process probabilities can be treated statistically. Modeling the dynamic evolution in time steps over a specified time horizon will be explored in a more advanced version.

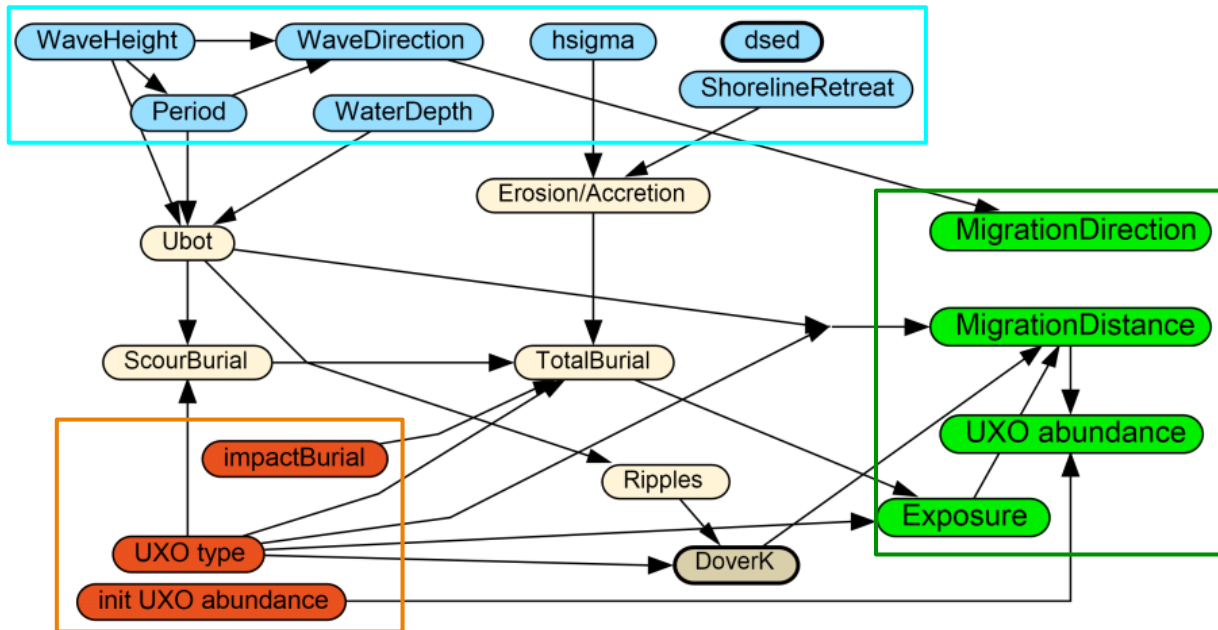


Figure 2.1. Diagram of the core Bayesian Network (BN) in UnMES modeling the burial and migration response in a given environmental setting (specified by blue nodes). Knowledge of the quantity, type, and initial burial condition of the munitions are provided in the orange nodes. The resulting predictions are found in the output (green) nodes.

2.1 Introduction to Bayesian Networks

The core construct of UnMES, the Bayesian Network (BN), sometimes called a Bayesian belief network [Pearl, 1988], is formed as a directed acyclic graph (DAG) of variables (nodes) connected by directed links (arrows). Each node represents a random variable and the links represent statistical dependencies between them. As the value at each node is a probability mass function, a BN is a method to model a multivariate domain that contains uncertainty. This uncertainty can be due to incomplete specification of the interactions governing the behavior of the domain, such as the simplification of wave orbital velocities using linear theory, or incomplete knowledge of the state of some of the variables, as when water depth is estimated from an old or poorly-sampled bathymetry. The uncertainty is

propagated through the BN by the probabilistic inference using Bayes theorem². Figure 2.1 shows the DAG of nodes that form the core BN of UnMES for a wave-dominated environment.

The BN portion of UnMES is designed and implemented using the commercial software package ‘Netica’ [Norsys, 2015], which provides a convenient user interface for graphically designing, building and modifying networks, as well as entering new input probabilities (“findings”) and displaying the resulting predictions. To represent the spatial variability across a contaminated underwater site, the core Bayesian Network is replicated at cells across a two-dimensional representation of the geographic region of interest as diagrammed in Figure 2.2. The overall structure is implemented in Matlab [MathWorks Inc., 2014], which interacts with Netica through its JAVA Application Programmer Interface (API). Further details are provided in Sections 2.2 and 5.

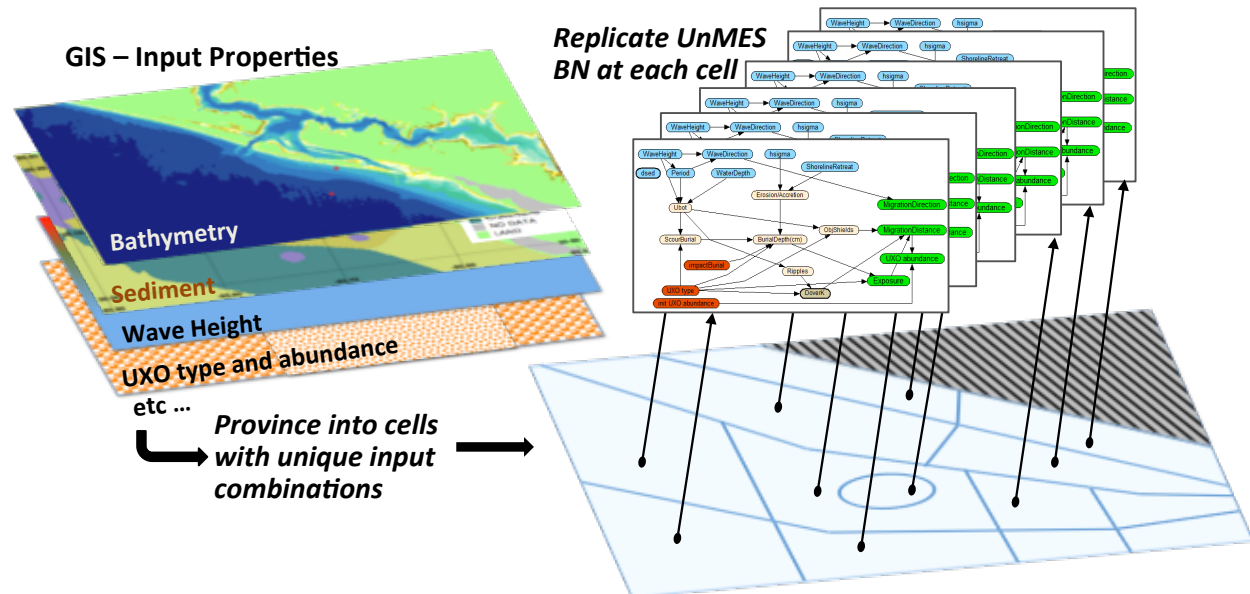


Figure 2.2 Conceptual illustration of GIS software framework for spatial implementation of UnMES.

After a Bayesian Network has been constructed, it can be applied to a particular situation by entering information (known as “evidence” or “findings”), setting the values of nodes that are known. For example, in UnMES, these nodes will include the environmental observations for a particular location. Then probabilistic inference (also called “belief updating” in a BN) determines new probabilities for the states of all the other dependent

² For background on Bayesian reasoning and its application to graphical models see Jensen and Nielsen [2007].

nodes. These are displayed in Netica as “belief bars” which show the shape of the probability distribution. Before performing belief updating, the BN must be compiled. For this, Netica uses an efficient junction tree algorithm based the assumption of conditional independence [Koller and Friedman, 2009]. In order to implement the inference algorithm in Netica, every node must be discrete with a finite number of states. Some nodes are naturally discrete, e.g. UXO type. However most environmental variables are inherently continuous, so that total range of the variable must be broken into a number of intervals, or states, whose sizes do not need to be constant. The intervals should be small enough to discriminate different response states, but not so narrow that the intervals have a higher resolution than the available data warrant and/or such that the computational requirement is prohibitive. The discretization choice for each node is an important part of the design process and will be discussed in more detail in Section 3 for the present UnMES application.

2.2 Nodes, Links and Conditional Probability Tables

A node in a BN with no links coming into it is considered a “parent” node, and will contain an unconditional probability table quantifying the probability mass function (PMF) over the states of the variable that it represents. In the UnMES, these parent nodes act as input variables, providing the boundary conditions for an environmental scenario, for example, the Wave Height and UXO Type nodes shown in Figure 2.1. If a node has one or more links pointing into it, it is a “child” node, and has a conditional probability table (CPT). Each entry in the CPT contains a conditional probability for a specific state of that child node, given a specific configuration of the states of its parents. In UnMES, there are also intermediate variables such as the computed Bottom Orbital Velocity, which is a child to the wave forcing nodes, and also a parent to the node ScourBurial.

A Bayesian Network can be used in diagnostic mode, i.e. findings can be specified at a “results” node (e.g. migration distance), and then the most probable configuration of values for the rest of the network can be determined. Another important diagnostic feature that Netica provides is the ability to do sensitivity analysis, producing a report of how much the distribution of states at a selected node could be influenced by a particular specified state at each of the other nodes in the net. The use of sensitivity analysis will be presented in the forthcoming Demonstration Report on the prototype UnMES implementation [Rennie and Brandt, 2015b]. Both this single-finding sensitivity analysis, and a comparison of results from inputs of varying levels of detail can identify which factors contribute the most to the predicted uncertainty. Because environmental data acquisition is often the most expensive part of a site remediation study, this evaluation, performed early in the process, would be important to help refine data requirements.

Relationships in the network are defined by each node's CPT, which is a multi-dimensional array that has one probability value for each combination of parent and child states. The CPT will be an N -dimensional table, where N is the number of parents, which has a total number of entries equal to $M_1 \cdot M_2 \cdot \dots \cdot M_N$, where M_i is the number of states in parent node i . The number of entries in the CPT will be the multiple of the number of child states times the number of states in each parent. Clearly, if variables are discretized into numerous intervals (states), the size of the CPT grows rapidly.

Most of the variables in UnMES describe physical processes and are continuous in nature. The choice of the discrete intervals by which to represent each node should correctly reflect the sensitivity of its response to its forcing, yet cover the range of interest in as few states as possible, so as to be represented by a compact CPT [Plant and Holland, 2011]. Note that there is no requirement that the intervals be the same size across the range of the variable. When designing UnMES, the resolution of the discretization interval reflects a trade-off between resolving important information and avoiding over-specification of details occurring at scales smaller than the expected uncertainty. The choice of state intervals is an important design decision; the rationale for UnMES state boundaries is detailed in Section 3.

Populating each of the entries in the CPT is the main effort in building the BN. Often CPT population in Bayesian Networks is accomplished by training on multiple data observations. An example application of BN to predict coastal response to sea level rise by Gutierrez *et al.* [2011] was trained on a large historical data set developed by the U.S. Geological Survey (USGS). As there are only a modest amount of observations relating to the migration and burial of underwater munitions, the CPTs in UnMES will be largely filled in by a Monte Carlo exploration over the domain of interest using simple deterministic process models. The deterministic models are “simple”, in that they are focused on capturing the first-order response, and do not attempt to replicate small details of the behavior, given our insufficient knowledge of the system. Available laboratory and field data is used to calibrate the parameters of these models [Rennie and Brandt, 2014]. The state of the deterministic models developed for use in the UnMES is described in Section 4.

2.3 Spatial Distribution: Replicas of the Bayesian Network

At UXO contaminated sites, managers may need to answer the question of whether certain areas within the site are more susceptible to munitions migration/aggregation or burial than others; or more specifically, what are the probabilities of UXO aggregation and burial

for local areas within the site of interest. Another prediction requiring spatial mapping occurs when regions of higher munitions contamination (i.e. larger abundance of UXO) are identified in the initial site conceptual model, or if there are sub-regions where the potential for human interaction is particularly great. To address these questions it is important to implement the UnMES in a 2-D spatial configuration that will naturally connect to map-oriented risk assessment products.

The application of Bayesian networks in a GIS framework for geospatial reasoning has been explored in several fields, including hydrology [USEPA, 2007], ecosystem modeling [Landuyt, *et al.*, 2015], and military logistics [Laskey, *et al.*, 2010]. However, the experience with implementation of this construct is relatively new, with no established software framework. Norsys is in the process of developing a product, GeoNetica, which facilitates the use of Netica Bayesian Networks in conjunction with raster-style GIS input and output. GeoNetica interfaces with multiple commercially available GIS systems and will be of great benefit for implementing the UnMES in coordination with the site-specific environmental GIS databases (Figure 2.2). GeoNetica is in “Beta” release to a limited customer base. Recently, JHU/APL was approved to join this initial test group. For this preliminary implement of UnMES, we will couple the UnMES Netica BN with the open-source Geographic Information System QGIS [www.qgis.org] to demonstrate the spatial framework analysis approach. Practical application of UnMES would require its integration into a GIS framework that meets the geospatial data standards required by the agency with cognizant authority for the contaminated property.

As with the continuous nodes in the BN, the spatial domain should be discretized into regions of relative uniformity, analogous with the nodes’ state intervals. As with the state intervals, the uniform geographic regions are not necessarily of all of the same size. Often spatial areas are partitioned into a uniform grid of evenly spaced regions (pixels), as in raster GIS format. This is a straightforward approach which is simple to work with, but can be inefficient, since large numbers of pixels may contain the (approximately) same feature value. The environmental data required by UnMES, such as bathymetry, is frequently available as a GIS raster layer, and should be preprocessed to a pixel resolution no finer than needed to resolve the state intervals in the corresponding BN node. Wave information from gridded coastal models is naturally stored in raster (pixel) form.

Preprocessing steps are necessary to prepare the GIS data before the input nodes of the BN can be populated. The several input layers must be reshaped for common pixel alignment and resolution. There are two approaches to implementing a BN in a GIS framework: a fast approach which is memory-intensive, or a slow one with less memory usage [Landuyt, et

al., 2015]. The slow mode is based on GeoNetica and runs the BN model at each pixel independently. For the fast approach, collections of pixels which represent unique combinations will be combined and referred to as a “cell”. There usually will be many fewer cells than pixels for a given site implementation. Then the BN is replicated at each of these smaller set of locations. This approach requires a catalog that lists all unique cells with their corresponding pixels, and then maps the probabilistic model output back into raster form. This catalog allocates considerable amounts of memory. However, the unique cell approach allows for customizing the nodes’ discretization intervals in the nodes for more efficient dynamic range coverage (Section 3). The advantages of each approach will be evaluated as we gain experience with implementation of UnMES at additional sites.

In the initial version of UnMES, the core BN is run for each cell of the joint GIS database independently. The probabilistic output is redistributed back through the catalog to the corresponding pixel locations in output GIS raster layers that can be displayed as maps visualizing the predictions and their corresponding uncertainty. The presentation of results can be displayed in several forms, including maps of most probable state (or mode state), accompanied by a map of the probability of that reported state; or a map of expected value along with a second map of standard deviation. A discussion of the methods of visualizing uncertainty is presented in Section 5.

2.4 Temporal Evolution

The process of UXO migration on the seabed is envisioned to be a repeated sequence of movement, then burial, followed eventually by re-exposure, leading to possible further movement. The ESTCP field tests conducted at the Field Research Facility (FRF) in Duck, NC [Wilson *et al.*, 2008a] observed surrogate UXO buried under sediment to depths several times the object diameter. Subsequent observations revealed these UXO were at different locations, but again deeply buried. It is inferred that local bathymetric change, either from bedform migration or shoreface adjustment, caused the UXO to become unburied, allowing the UXO to migrate, and then rebury. Based on a compilation of field test results from SERDP researchers [Calantoni *et al.*, 2015, Traykovski, 2015] as well as modeling studies by Jenkins *et al.* [2013], burial is by far the most probable state of the UXO at any given time, with re-exposure and movement occurring very infrequently at most sites. However, it may be just these unusual events that are of most concern to site managers. At many of the sites, the munitions have been in residence for years, if not decades. The potential for infrequent events to occur, though small, is finite.

The approach taken by UnMES is to model the burial-migration cycle, not explicitly as a time-stepped sequence of processes, but as the combined probability of burial and motion states, given a long-term distribution of environmental forcings. We focus here on a wave-forced environment, so the temporal distributions of wave heights and their corresponding periods are required input, along with a quantification of the probability of changes in seabed elevation that provide the potential for re-exposure. The time scale of temporal evolution is implicit in the duration over which the statistics are derived. For example, if the distribution of seabed elevation changes are computed from measurements or modeled processes representing weeks or a few months, that PDF captures re-exposure potential due to local bedform migration, but not that caused seasonal shoreface adjustment, which occurs over annual time scales.

3 Details of Nodes in UnMES

The nodes in the core UnMES BN can be grouped into three sets. In a predictive mode, normally the input nodes which specify the geologic and meteorological setting (shown as blue in Figure 2.1), will have their states set using values from the GIS environmental database. There are several variables, denoted by orange, that provide existing knowledge of the initial disposition of the UXO that are contaminating the site, such as the kinds of munitions and their relative abundance.

The probability distributions resulting in the output prediction nodes (green set shown in Figure 2.1) contain the information that will feed into site manager risk assessment tools. The set of intermediate nodes is where the functionality of UnMES lies. The CPTs for these nodes are filled in using our knowledge of ocean physics along with recent laboratory and field research into the behavior of munitions on the seabed in the form of process models (see Section 4) and rule based expert input for situations where physics based models are not available.

A crucial step in constructing the BN is the choice of discretization intervals for both the input and intermediate nodes. The primary determinant of the discretization choice is the need to adequately resolve the behavior of the UXO. However, in order to maintain a reasonable size for the multi-dimensional CPTs, there is a need to limit the number of discretization intervals. For sufficient discrimination of the munitions burial and migration patterns, a large number of states may be required, but the inherent uncertainty of input measurements should be considered before creating unrealistically high-resolution intervals. Whitehouse [1998] cites typical uncertainties, ranging from 10% to 20% for the input environmental parameters in UnMES, when there has been an in-situ field survey. So

the uncertainty when using generic regional predictions can be expected to be significantly larger.

The precision with which UnMES needs to predict burial is determined by a number of factors. Doctrinal burial categories used in the Navy's Mine Warfare and Environmental Decision Aids Library (MEDAL), which reflect the sensitivity of various underwater mine-hunting sensors, are set to intervals with boundaries of 10%, 20%, 75% and 100% burial. In addition to supporting sensor performance prediction, UnMES also calculates when UXO are buried sufficiently so that mobility is suppressed. The percentage burial at which this "lockdown" occurs has been estimated to be between 40% to 50% [Wilson *et al.*, 2008a]. Therefore the scour burial states of 10%, 20%, 50%, 80% and 100% of the UXO diameter are proposed for the initial version of UnMES. These discretization intervals are denoted on Figure 3.1, and listed in column 1 of Table 3.1.

Table 3.1 Discretization Intervals for some UnMES Bayesian Network Nodes

Scour Burial (%)	Bottom Velocity U_{bot} (cm/s)	Water Depth h (m)	Wave Height (m) for $h=2.5\text{m}$	Wave Period (s) for $h=2.5\text{m}$	Wave Height (m) for $h = 7\text{ m}$	Wave Period (s) for $h = 7\text{ m}$
< 10	< 10	1 to 1.5m	< 0.3	< 4	< 0.4	< 4
10 to 20	10 to 20	1.5 to 2m	0.3 to 0.4	> 4	0.4 to 0.7	4 to 6
20 to 50	20 to 30	2 to 2.5m	0.4 to 0.5		0.7 to 1.0	> 6
50 to 80	30 to 40	2.5 to 3m	0.5 to 0.65		1.0 to 1.4	
80 to 100	40 to 50	3 to 4m	0.65 to 0.8		1.4 to 1.7	
fully buried	50 to 60	4 to 5m	0.8 to 1.0		1.7 to 2.0	
	60 to 75	5 to 6m	1.0 to 1.2		2.0 to 2.5	
	75 to 90	6 to 8m	1.2 to 1.4		2.5 to 3.0	
	90 to 105	8 to 10m	1.4 to 1.7		3.0 to 3.5	
	105 to 120	10 to 15m	1.7 to 2.0		3.5 to 4.0	
surf zone	120 to 160		2.0 to 2.6		4.0 to 5.3	
			> 2.6m		> 5.3 m	

The functional response to forcing is highly sensitive for many of the relationships modeled here, but the domain of strong sensitivity to one variable can change depending on the value of a second variable. This will be illustrated in detail for the Bottom Velocity node in the following section. Because the UnMES GIS framework creates a new instance of the BN at each spatial cell, we can take advantage of the reduction in dynamic range for variables that are constrained within that spatial region, such as water depth and sediment grain size. For example, because waves break in water depths on the order of their height,

the Wave Height node for the BN replica at spatial cells in very shallow water need not include states for the larger wave heights that may be found farther offshore.

In a previous implementation of a Bayesian network to predict mine burial [Rennie *et al.*, 2007] the CPT was defined using an off-line Monte-Carlo computation of a predictive deterministic model. For UnMES, several of the deterministic models (see Section 4) are simple enough to specify the equation defining the relationship directly in Netica's node Equation box whereby Netica's Equation-to-Table option can be used. The Equation-to-Table option performs a similar Monte-Carlo sampling of all states on-the-fly to build the table internally. This makes it possible to construct each BN replica in a custom manner for each spatial cell in the joint GIS database (See Section 3.3.2).

3.1 Rationale for Discretization: Bottom Velocity

The bottom velocity (U_{bot}) is an intermediate node that acts as a parent to both the burial and migration nodes. Velocity at the bottom of the water column is the peak orbital velocity computed from linear wave equations [Soulsby, 1997], as a function of the value of the input states: Wave Height, Period and Water Depth. To determine the appropriate choice of state interval width for the Bottom Velocity node, the sensitivity of the parameterized model for scour burial is considered. This model was the focus of recent studies [Rennie and Brandt, 2014], reviewed in Section 4.1.

Across a given spatial cell, the sediment characteristics are fixed to a single value. In Figure 3.1, scour burial, %B (in percent) is plotted against increasing bottom velocity for two sediment values, and for two different UXO shapes. The type “bomb” is used to represent a larger cylindrical UXO, nominal diameter of 150 mm, and “shell” denotes artillery with a tapered shape of nominal diameter 80 mm. The model for %B is dependent on the parameter θ , the sediment Shields number [Friedrichs, 2014], which is a function of the sediment grain size and U_{bot}^2 . The “bomb” curves show the relationship $\%B = 100 \cdot 2.2 \cdot \theta^{0.85}$, the best fit parameters found from the data on cylinder burial in Rennie and Brandt [2014]. The two sediment sizes bound most of the range of sand grains, from $d_{\text{sed}} = 0.2$ mm (very fine sand) to $d_{\text{sed}} = 0.8$ mm (coarse sand). The “shell” curves show $\%B = 100 \cdot 5 \cdot \theta$, the empirical fit based on the burial of tapered shapes. At cells with the very small grain size, burial is highly sensitive to bottom velocity, especially for the “shell” burial with the larger scale factor applied. However, for a “bomb” in coarse sand, it takes a sizable increase in bottom velocity to cause substantial burial.

To understand burial behavior to the precision proposed in Table 3.1, U_{bot} should be resolved to within approximately 0.05 m/s intervals for a cell with a sediment type of very fine sand (red and black lines in Figure 3.1). For a BN with d_{sed} set to coarse sand, the velocity intervals could be as wide as 0.15 m/s. In addition to considering the resolution required to discern changes within the deterministic relation, the uncertainty of the empirical fit (Section 4.1) should be considered. Overlaid on Figure 3.1 are the 95% confidence ranges (dashed lines) for the empirical fits for burial behavior of the two UXO shapes. Because there were very few sample data points for the tapered shapes, the uncertainty is noticeable larger for the “shell” relationship. Taking the 95% confidence ranges into account, a velocity interval of 0.10 m/s accurately reflects current knowledge of the percent burial relationship with U_{bot} . These Bottom Velocity intervals are indicated by marks along the left half of the x axis in Figure 3.1.

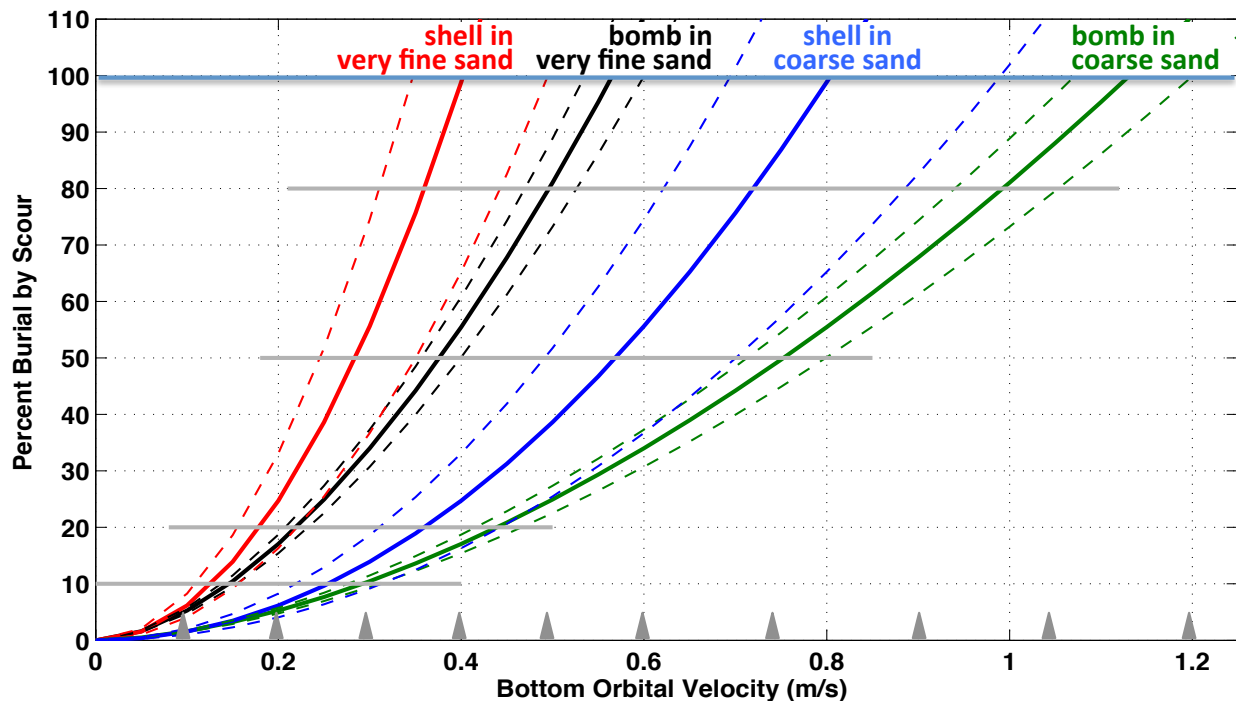


Figure 3.1 Scour burial as a function of bottom velocity for a bomb-like object, and for a tapered shell. The green and blue lines show burial in coarse sand, and the red and black lines show burial in very fine sand. The dashed lines indicate 95% confidence about the slope parameter from empirical fits. The grey horizontal bars delimit the scour burial state boundaries at 10%, 20%, 50%, 80% and 100%. Grey triangles mark U_{bot} state intervals.

For velocities ≥ 1.2 m/s, the slowly-burying munitions will become fully buried even in coarse sands. This discrimination interval of larger U_{bot} is of interest for estimating migration (Section 3.7) in the situation where erosional processes have unearthed the UXO. Because our knowledge of migration distances is limited, the choice of wide U_{bot} intervals at

the higher speeds is appropriate. With bottom orbital velocities above about 2 m/s, the wave starts to break, and linear wave formulation is no longer applicable. The physics of water motion in the surf zone is extremely complex, and for the present we will simply assign a “high” value to U_{bot} for these conditions. For the initial version of UnMES, we set the state interval widths for U_{bot} at 0.1 m/s up to 0.6 m/s, increasing to 0.15 m/s widths up to 1.2 m/s, followed by 0.4 m/s interval to 1.6 m/s. All larger values will be denoted “surf zone” and assigned $U_{bot} > 2.0$ m/s, as shown in Table 3.1. These state intervals are illustrated in Figure 3.2 where the nodes are expanded to show their “belief bars”, the method that Netica uses to display the updated PMF at each node. Note that the Wave Height distribution represents the temporal variation within a given GeoNetica cell, while Water Depth remains fairly constant within the cell. Further discussion of Figure 3.2 is presented in Section 5.

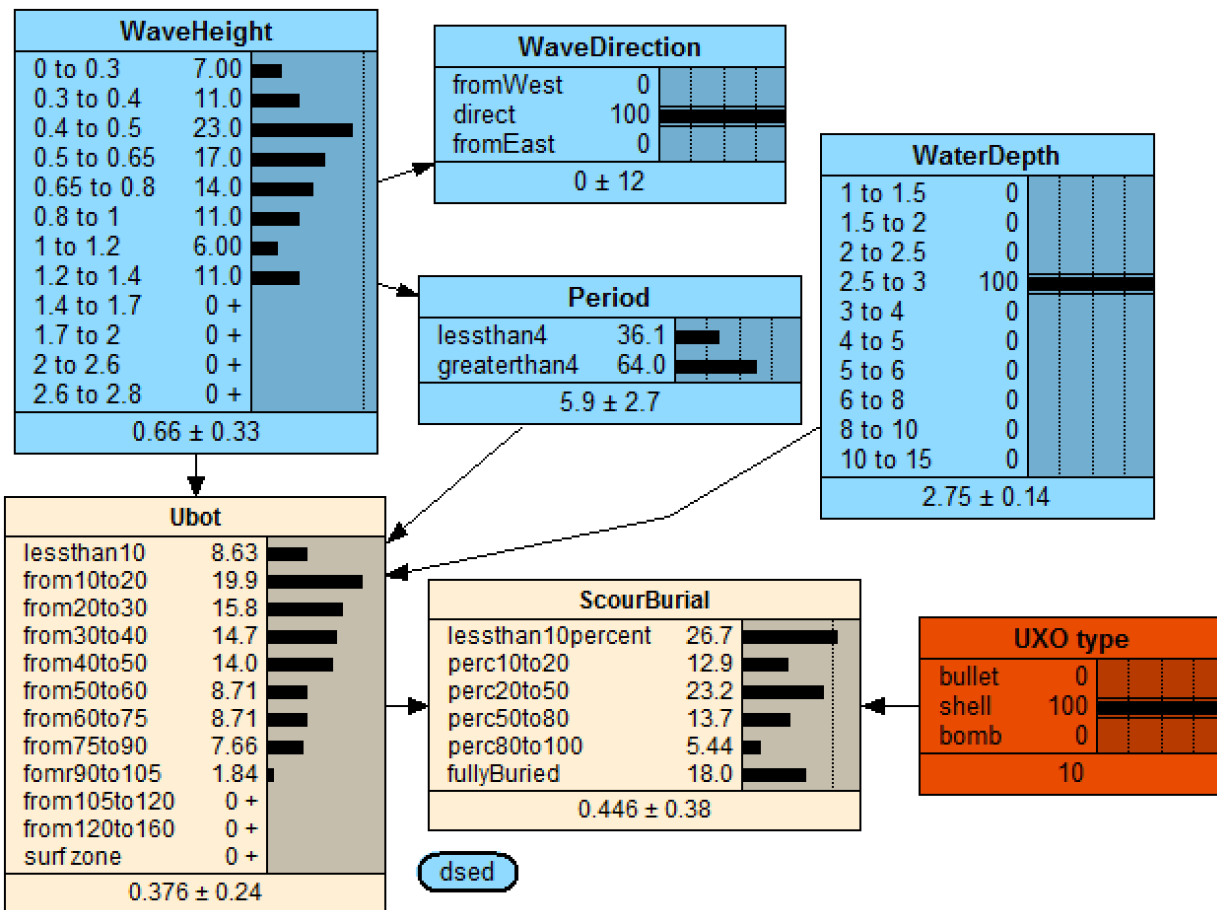


Figure 3.2 Netica BN for scour burial. Representative beliefs bars of the BN nodes for waves, water depth, bottom orbital velocity and percent burial by scour, showing the discretization choices defining the state intervals. Water depth is set to 100% belief for the BN replica within a spatial cell defined by isobathic depths between 2.5 and 3 m. The UXO Type node is set to represent an area where all underwater munitions are similar to naval artillery shells.

3.2 Input Nodes: Geologic Setting

The geological characteristics of the location are specified in the UnMES by a node specifying the sediment grain size, d_{sed} , along with a bathymetric variable, the node WaterDepth. A third node, called h_{sigma} , quantifies the vertical variability in bathymetry about the mean water depth, h . These variables are assumed to vary over the spatial domain, but are temporally static. Sediment grain size will be constant within a given cell, while the temporal variability of h is captured in the h_{sigma} statistic. The map region to be modeled is partitioned into cells based on the merged GIS raster layers for these variables, as discussed in Section 2.2 so that in each cell, these nodes have a fixed value; i.e. the input PMF is 100% in a single state. By narrowing the range of several input (parent) nodes, the size of the CPTs of the intermediate (child) nodes is reduced.

3.2.1 Sediment characterization

The characteristic of the sediment is given by a single parameter, d_{sed} , the diameter of the sand grains in mm. At sites of interest, a sediment analysis would usually be performed, where separation by sieving results in the PMF of sand grain size (e.g. Wilson *et al.*, 2008a). Because the scour process is sensitive to sediment size (as seen in Figure 3.1), the details of the grain size distribution were shown to play a role in CFD studies of UXO burial [Jenkins *et al.*, 2012]. The UnMES approach is focused on first-order effects, under the assumption that the overall uncertainty (due to imperfect knowledge of the location and history) renders details irrelevant. Therefore the grain size distribution is represented by its median value. This value is treated by Netica as a constant, rather than a state with a given interval width, so no discretization choice is required for d_{sed} . Note that nodes in Netica which represent constants do not require links, but are available as input to all other nodes.

For many U.S. coastal areas, there is sediment database available from NAVOCEANO. A map of the NAVOCEANO Bottom Sediment Type data, forming a QGIS raster layer, is shown in Figure 3.3 for the vicinity of Panama City, FL. In many wave-dominated locations, the sand will be fairly well sorted by the wave action, so that water depth and sand grain size are inversely correlated. However, due to geologic history, outcroppings of different sediments can occur, as seen in Figure 3.3, where pockets of gravel and shell are interspersed.

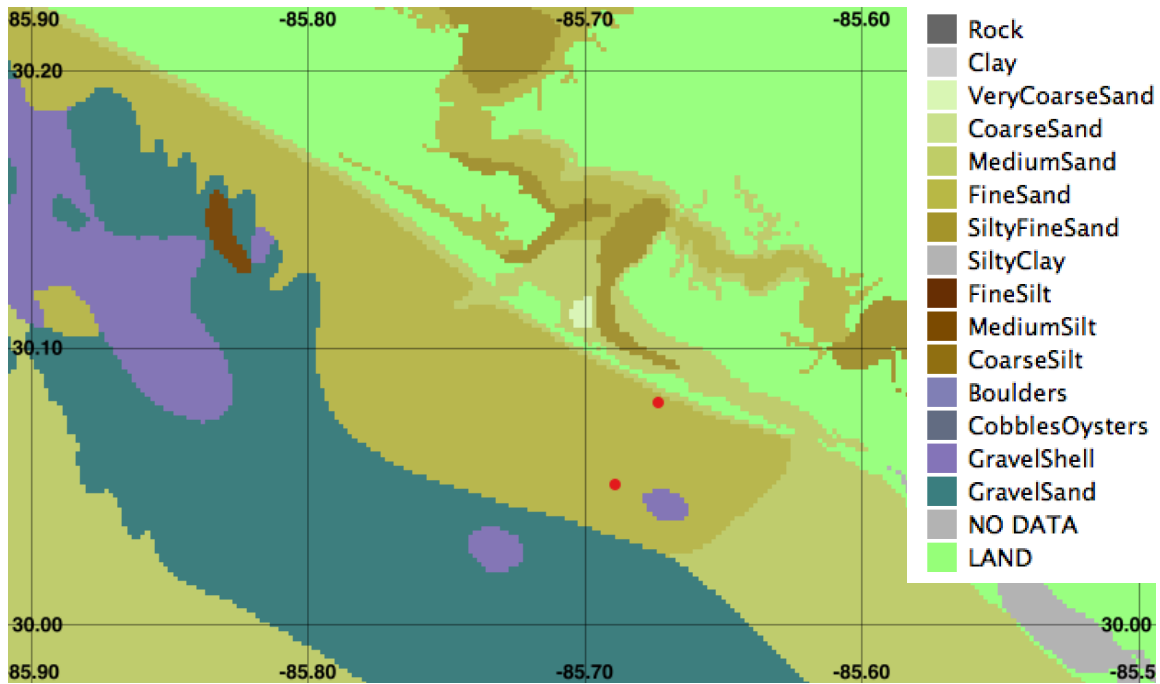


Figure 3.3 QGIS map of bottom sediment type from NAVOCEANO database from the region in the Gulf of Mexico near Panama City, Florida. The sediment type can be mapped to a median sand grain size, which is assumed to not vary with time. Red circles mark the locations of the TREX13 field experiment locations [Calantoni, 2015].

3.2.2 Water Depth

Coastal bathymetry is generally available at all U.S sites at a minimum as charts from NOAA's Office of Coastal Survey and digitally from the from the National Ocean Service (NOS) hydrographic survey archive. Another source is the U.S. Naval Oceanographic Office (NAVOCEANO) Digital Bathymetric Data Base – Variable Resolution (DBDB-V) product. These archived bathymetries can be used as a baseline. At most sites of interest, at least one high-resolution survey should have been performed to provide more detailed bathymetry. At many locations, repeated surveys allow an assessment of bathymetric variability which is crucial to predicting the likelihood of re-exposure of previously buried munitions. Models of dynamic coastal morphology [Hanson *et al.*, 2003, Jenkins and Inman, 2006] can be employed to estimate the variability if historic measurements are not available. For the preliminary BN, the variability is specified as a standard deviation of vertical variation (h_{σ}) about the local mean depth at each cross-shore location (see Section 3.5). This statistic could be derived from repeated surveys, or computed from Monte-Carlo exploration of models of cross-shore profile evolution in response to regional wave climatology.

Determining the appropriate width for the state intervals of the `WaterDepth` node requires the consideration of both the measurement accuracy of h and the sensitivity of the child node U_{bot} . The average vertical resolution of bathymetry across the region of interest varies according to its source. Modern bathymetry derived from airborne lidar should achieve accuracy of 0.15 m, however, substantially more areas are covered by hydrographic surveys, where recent standards for sonar soundings only require a vertical uncertainty of less than 0.5 m in shallow (< 100 m) areas [Wells and Monahan, 2002]. There is a corresponding increase in horizontal resolution available from coastal lidar studies (pixel size of 2 to 3 m²) higher than that available from archived hydrographic sources (on the order of 100 m²). Figure 3.4 shows an example QGIS raster layer of water depth formed from a combination of hydrographic and lidar sources. The bathymetry shown illustrates this discrepancy in resolution: the regional bathymetry is taken from DBDB-V which has 3 second resolution, i.e. pixels every ~ 93 m. A subsection of the nearshore region (the beach out to less than 8 m depth), is formed from lidar data taken in 2005, in a USACE Joint Airborne Lidar Bathymetry Technical Center of Expertise (JALBTCX) survey after Hurricane Katrina, which has resolution of close to 2 m², and vertical accuracy between 15 to 30 cm [Guenther *et al.*, 2000].

The bottom orbital velocity is proportional to the reciprocal of the square root of h (given the same wave height), therefore U_{bot} varies slowly in relatively deep water. For $h > 7$ m, it requires a decrease of over 2 m to cause an increase in U_{bot} larger than the state intervals specified in Table 3.1. In very deep water, the width of the interval can be even larger. However, in shallow water, the orbital velocity becomes substantially more sensitive to changes in h , so that the water depth interval must be as small as 0.5 m to resolve U_{bot} sufficiently. The choice of state intervals for the `WaterDepth` node are listed in Table 3.1 and illustrated in Figure 3.2. Note, again, that the value of h is considered to be fixed in time. Also, for any given spatial cell, the value lies completely within a single state interval; in fact, that is how the boundaries of that spatial cell were defined (see Section 2.2). The color scale in Figure 3.4 uses the water depth state intervals, so that the color changes delimit the isobars where there is a state change.

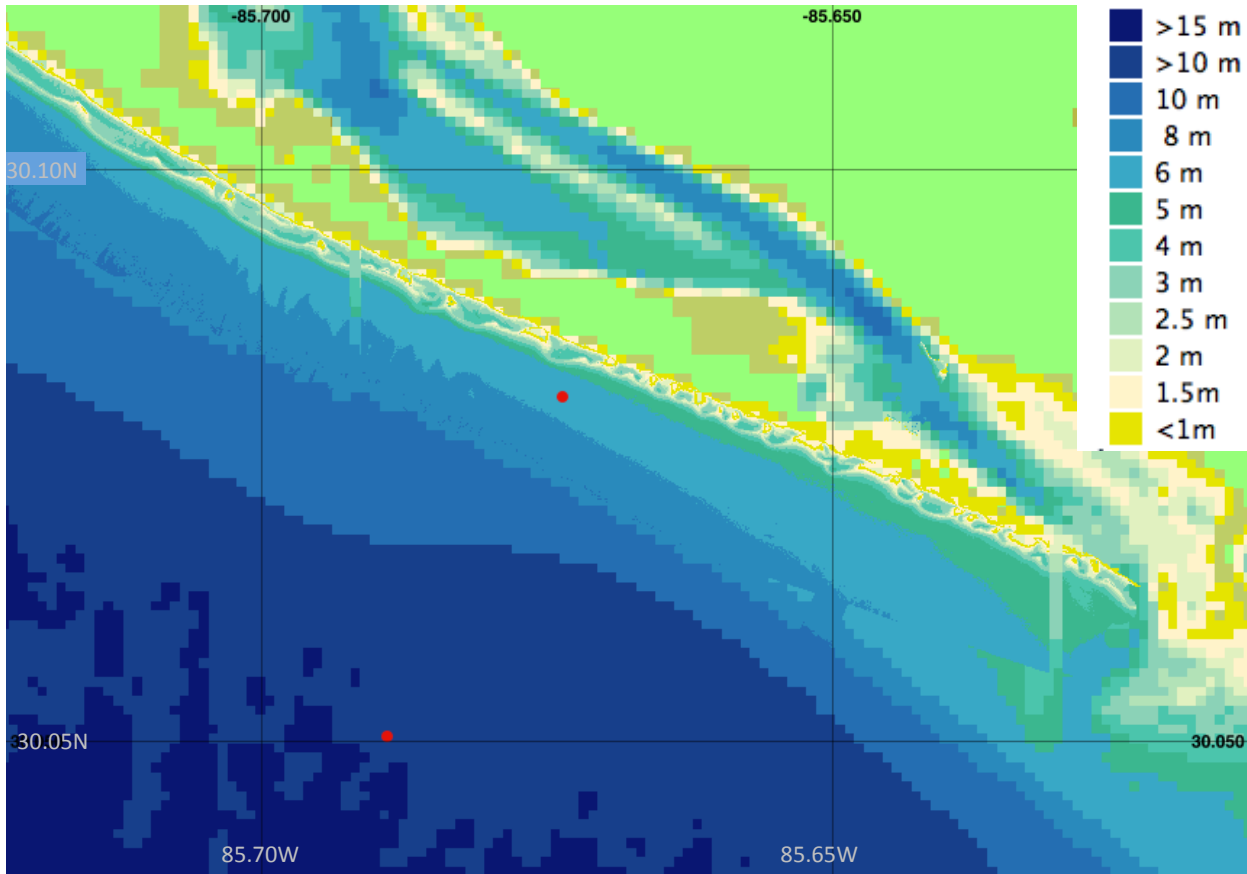


Figure 3.4 Water Depth near Panama City, Florida. Large scale bathymetry from DBDB-V. High-resolution near shoreline from 2005 survey by USACE JALBTCX. Red dots mark the locations of the TREX13 field experiment locations [Calantoni, 2015].

3.3 Input Nodes: Wave Forcing

The nodes describing the characteristics of wave forcing must capture the temporal variation of the dynamic forcing which causes UXO burial and migration. The input PDF of wave heights should be computed as a histogram over a time period that is long enough to be representative of the conditions at the site. For the probabilistic approach taken by UnMES, the exact burial-motion sequence phasing (Section 2.3) is assumed to be unimportant; therefore, for adequate statistics, the PDF should be developed over a time period encompassing multiple cycles of burial-motion as well as multiple cycles of wave patterns (diurnal, seasonal, annual). Figure 3.5 shows an example histogram of wave height computed from 8 years of wave buoy measurements offshore of FRF at Duck, NC [FRF, 2011]. Note at any moment in time an entire spectrum of waves is present; the single

statistic represented here is significant wave height, H_{sig} , computed as 4σ of the sea surface elevations measured during the measurement window (usually $\frac{1}{2}$ hour).

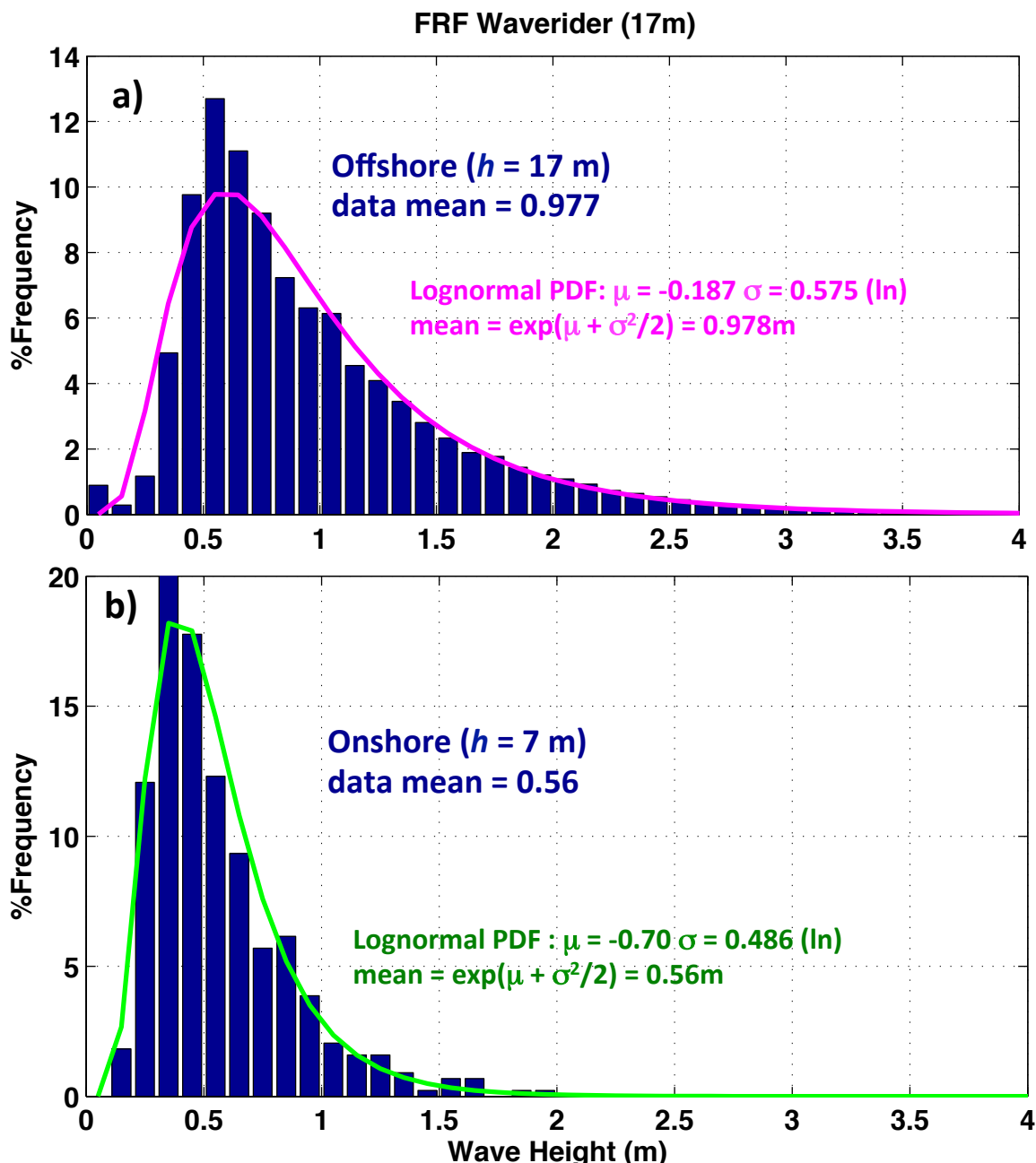


Figure 3.5 Probability distribution of significant wave height computed from measurements at the FRF Waverider buoy: a) shows the histogram of wave heights measured at a location in a water depth of 17 m during the years 1998 to 2006 with magenta line the best fit lognormal distribution. b) transformed wave heights at 7 m depths; green line is the best fit.

3.3.1 Shallow Water Wave Transformation

For most coastal locations, instruments measuring wave conditions are located offshore in deep water. Many U.S coastal sites are serviced by offshore wave buoys maintained by National Data Buoy Center (NDBC), part of the National Oceanic and Atmospheric Administration (NOAA). Offshore wave model predictions are available at locations in between buoys from the operational wave model WAVEWATCH III (Tolman, 2009), with hindcast re-analyses archived back to 1999. To populate the cells of the GIS framework for UnMES, which is generally most concerned with shallower regions close to shore, the transformation of the shoaling waves must be computed. NOAA's National Centers for Environmental Prediction (NCEP) is currently developing the Nearshore Wave Prediction System (NWPS) to provide high-resolution nearshore wave products [van der Westhuysen, 2012]. Until NWPS is routinely operational, the shoaling of deep-water waves to the shallow region of most interest to UnMES will require using a gridded nearshore wave transformation model such as SWAN, which was developed at Delft University and is being incorporated into NWPS [Settelmaier *et al.*, 2011], or the US Army Corps of Engineers (USACE) model STWAVE [Smith *et al.*, 1999].

Figure 3.6 illustrates the effect of shoaling on two waves approaching the beach at FRF, apply the wave-evolution model by Thornton and Guza [1983]. The water depth (in brown) shows a pronounced longshore bar at 200 m offshore, then increases with a slope of about 0.008 out to the depth of 8 m where a wave gauge is located. An offshore wave height of 2.4 m is plotted in dark blue; this wave can be seen to steadily decrease in height as it moves inshore, its energy dissipating due to the combined effect of bed friction and depth-induced breaking. At the crest of the longshore bar, this wave breaks, losing height rapidly, then continuing with H_{sig} about 0.75 m to just before the shore. In comparison, a wave in 8 m with $H_{sig} = 0.72$ m, shown in cyan, does not dissipate, but experiences slight H_{sig} growth as the shallower depths slow the wave, reducing its wave length, causing a compensating increase in height. Breaking again occurs at the crest of the longshore bar. Overlaid on Figure 3.6 are dashed vertical lines marking the discretization intervals for the water depth parameter determined in the Section 3.2.2. It can be seen that in order to spatially resolve the nearshore, closely-spaced cells are required. However, the near-surf-zone is a region of large uncertainty, so that such high resolution may not be warranted.

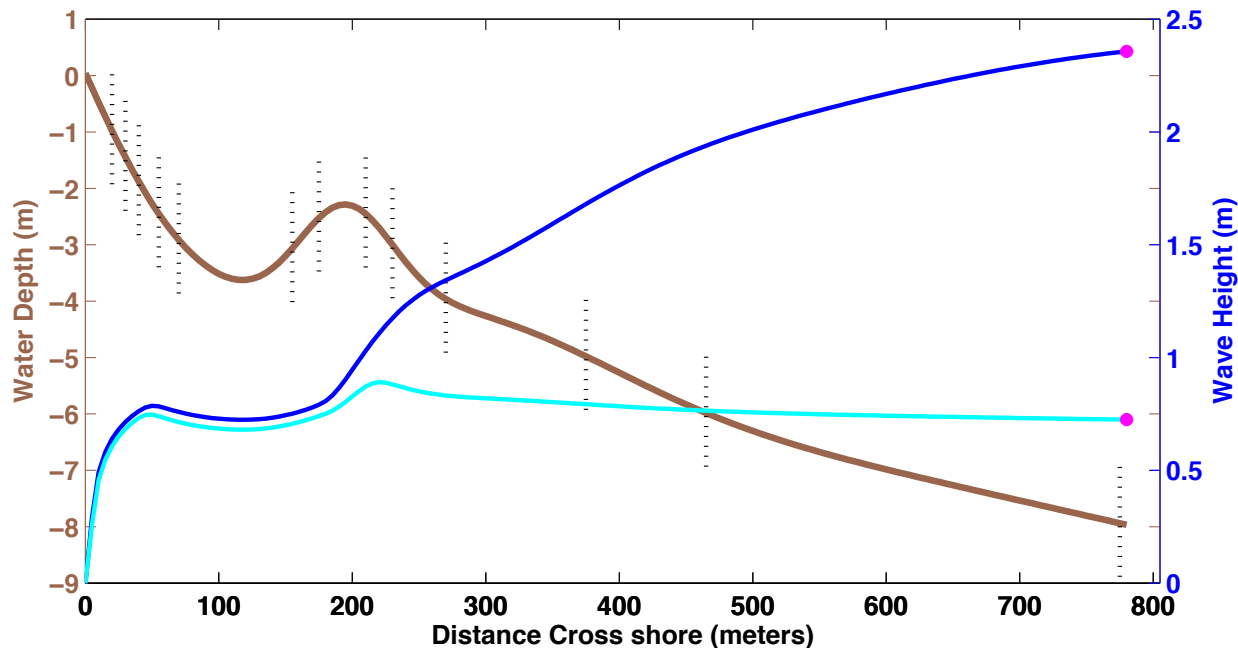


Figure 3.6 Cross-shore bathymetry and shoaling wave heights at FRF, Duck NC. Two example waves are shown with offshore heights of 2.4 m and 0.7 m (marked by magenta dots).

The use of Bayesian networks to model wave evolution from offshore into the surf zone has been explored [Plant and Holland, 2011] and, in the future, UnMES could be expanded to handle that portion of the required modeling effort. For the current version, it is assumed that wave characteristics at all spatial cells are determined offline, and provided to UnMES as an input PDF.

When modeling a single location, the prior distribution of the H_{sig} input node can be approximated using a histogram such as shown in Figure 3.5. To provide wave information for all the cells in a spatial implementation of UnMES, it is more practical to represent the PDF of H_{sig} parametrically, by fitting the observations to a parametric continuous probability distribution using maximum likelihood estimation. Then the GIS input consists of one or two layers of the appropriate parameter values. Netica provides an extensive library of built-in functions, including many analytic probability distributions. Wave formation via energy cascade is a multiplicative process; wave heights are all positive values and their distribution is highly skewed, with a low mean value but a large variance. Therefore the lognormal distribution is a reasonable approximation, requiring two parameters, μ , and σ . Overlaid on Figure 3.5a in magenta is the best fit lognormal distribution for the wave heights observed at the offshore FRF buoy in 17 m depth. The green line in Figure 3.5b shows the wave height distribution after application of the

Thornton and Guza [1983] shoaling transformation for a nearshore location with a water depth of 7 m. The lognormal parameterization is satisfactory for representing the bulk of the wave distribution at this site. In order to precisely model the tail of the distribution (the largest wave heights), which represents the most important forces driving burial, the use of an exceedance probability formulation will be investigated.

3.3.2 Discretization of Wave Height and Period

For fixed water depth h , bottom orbital velocity is approximately linearly proportional to wave height, $U_{\text{bot}} = m * H_{\text{sig}}$, with a secondary dependence on wave period T . The slope m approaches 1 in shallow water ($h \leq 2$ m). This strong sensitivity of the child node U_{bot} to changes in H_{sig} constrains the state intervals of the WaveHeight node to be fairly small. At a given spatial location in UnMES, h is considered fixed, but wave height and period will vary over time. Figure 3.7 illustrates the sensitivity of U_{bot} to H_{sig} and T for two water depths. In Figure 3.7a the depth is shallow ($h = 2.5$ m) and U_{bot} is seen to increase rapidly with H_{sig} , with $m = 0.6$ at $T = 3$ s, up to $m > 0.9$ for $T > 6$ s. To resolve this relationship requires very small state widths for the WaveHeight node, with H_{sig} intervals as small as 10 cm. However, the maximum wave height in the CPT is only 2.6 m; all larger waves are breaking (plotted as white), and can be assigned to the “surf zone” category. There is very little dependence on wave period, so that node can adequately be represented by only two states, below and above $T = 4$ s. This H_{sig} discretization for a shallow water depth is illustrated in Figure 3.2 and marked by the black arrows along the x-axis of Figure 3.7a.

In deeper water with $h = 7$ m (Figure 3.7b), U_{bot} increases more slowly with H_{sig} ; m ranging from 0.15 to 0.5. The maximum H_{sig} to delimit is 7.6 m; all larger waves would break before reaching this depth. The state interval boundaries for H_{sig} are computed at the U_{bot} interval contours (plotted in white) for the wave period ($T = 6$ s), which is the mean T for the example Gulf of Mexico location shown in Figures 3.3 and 3.4. The variation over wave period at this depth will be captured with three states. Note that wave period is invariant; it does not change as the waves shoal towards shore, and can therefore be represented by the same distribution at every cell. It is clear that, given local water depth, the BN at each spatial cell can be designed to adequately resolve the relevant wave height forcing using the number of intervals that were chosen for the bottom velocity node. The resulting choices of state intervals are listed in Table 3.1 for the two example water depths. In this manner, the CPTs for the nodes’ relationships can be represented using a manageable number of entries.

3.3.3 Wave Direction

Due to refraction, shoaling waves are constrained to increasingly be directed toward the shoreline (angle $\angle = 0^\circ$). Because it has been shown in some locations that shore erosion is sensitive to directional changes in the incoming waves [Ruggiero *et al.*, 2006] an input node for the incident angle is included in UnMES. Also, the longshore current direction is driven by this angle and used for predicting the UXO migration direction. Measurements of wave direction are not available as readily as those for height and period. The percentage of waves that approach obliquely from either the east or the west (assuming a shoreline along constant latitude) may be estimated from beach observations including video monitoring [Holman and Stanley, 2007]. In this version of the UnMES the wave direction parameter is used as a general indicator, therefore a coarse discretization of 3 states is chosen, with the state boundaries at $\angle = \pm 20^\circ$.

3.4 Input Nodes: Distribution of UXO

3.4.1 UXO Type & Abundance

The exact composition of munitions at a site is usually not well known. However an estimate of the type of munitions present is critical to the prediction of the current state of UXO burial and accumulation as their size, shape, and density affect burial and migration behavior. The size of munitions of interest ranges from small 20 mm bullets, through projectile shells and mortars with diameters from 40 to 81 mm, and howitzers as large as 155 mm. Diameter, length and weight data for common Naval munitions are readily available, and several studies have relied on estimating density by assuming a cylindrical shape. However many UXO of concern have more complex shapes. (Access to additional munitions details in DoD restricted ordnance databases will be beneficial for the development of UnMES.) Preliminary site surveys can provide a prior probability for the input nodes for UXO Type and UXO Abundance. At some sites, such as Camp Perry, OH, there are historical firing documents that allow estimates of the likely artillery areal concentration [Wilson *et al.*, 2008b]. In this version of UnMES, UXO Types include the category “bullet” with a diameter of 22 mm and a high density (specific gravity, $Sg = 7$). The type “shell” is assigned an intermediate diameter of 10 cm and is considered to have a tapered shape and moderate density ($Sg = 4.5$), while “bomb” represents a larger, cylindrical UXO with $Sg = 2.7$. Figure 3.2 illustrates the UXO Type node instantiated with 100% of the type “shell”.

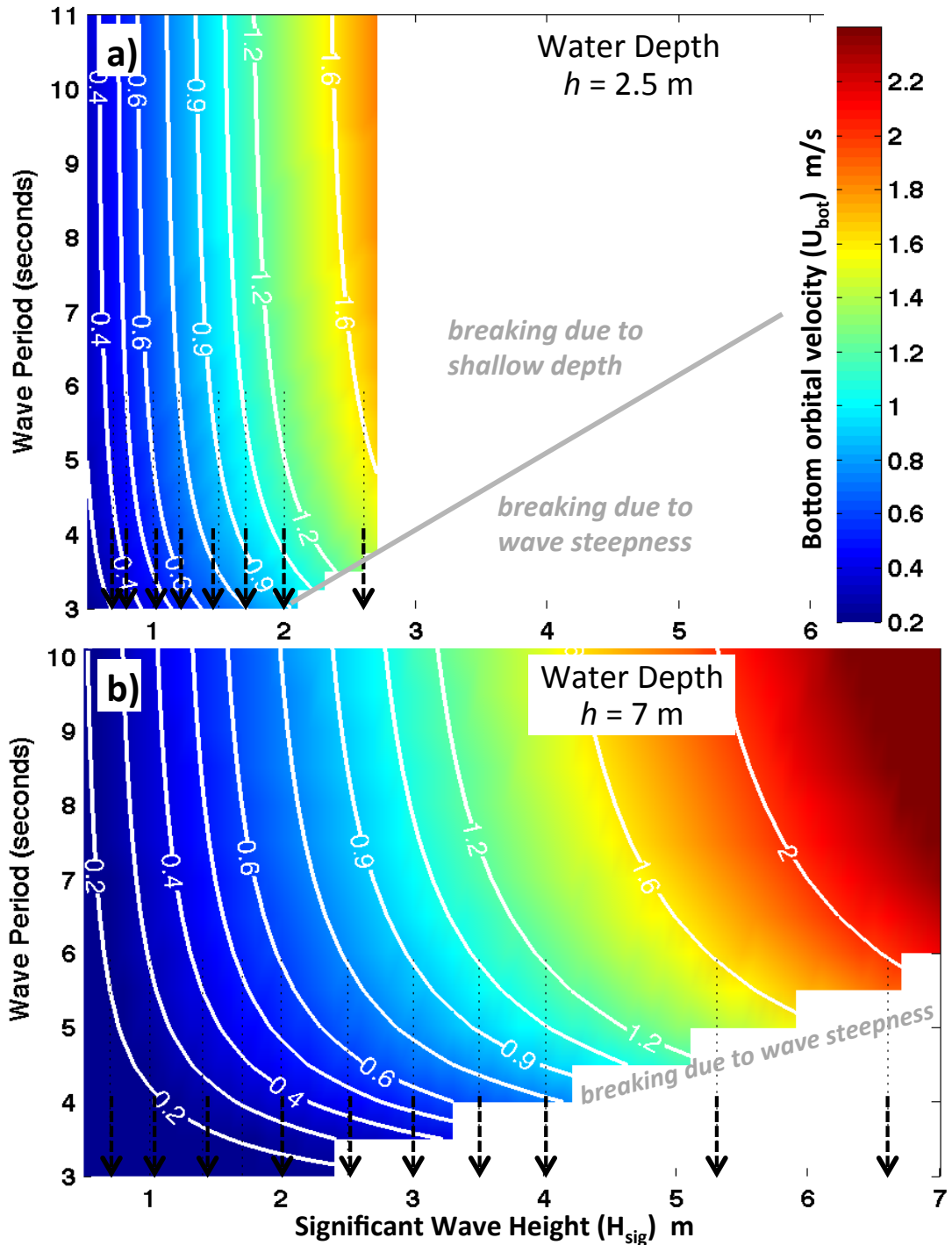


Figure 3.7 Bottom orbital velocity U_{bot} as a function of wave height H_{sig} and wave period at two example water depths: a) $h = 2.5$ m and b) $h = 7$ m. The black arrows mark the state interval boundaries required to discretize H_{sig} with adequately resolution in U_{bot} .

3.4.2 Initial Burial

The possibility of burial upon impact in sandy sediments is very low for munitions that were dumped at sea off a ship, based on research performed for the ONR Mine Burial program [Rennie *et al.*, 2007]. The hardness of a sand seabed, usually measured as sediment shear strength, is quite high (>12 kPa), and the impact velocity of ship-dropped munitions is usually low, less than 10 m/s. However, air-dropped bombs or fired artillery shells could have impact velocities exceeding 100 m/s. Future work will investigate the use of a proposed model for high-velocity sediment penetration [Chu *et al.*, 2011]. In the current version of UnMES, the Impact Burial node is a placeholder, indicating minimal burial (i.e., the state “less than 10%” instantiated).

3.5 Input Nodes: Probability of Erosion or Accretion of Sediments

The node Erosion/Accretion in the BN represents our knowledge of changes in the seabed level on spatial scales larger than the immediate area around the UXO. There are several mechanisms under investigation that could cause buried munitions to re-surface or be excavated. Most of these mechanisms also have the opposite potential and can bury the munitions by covering them with sediment. At very long time scales, the shoreline erosion is an obvious mechanism that can expose previously buried objects. Within an annual time frame, the dominant process on many coastal regions is the shoreface equilibrium profile adjustment to seasonal variation in wave climate. At many wave-dominated coastal nearshore sites, the evolution of surf-zone sand bar position is the largest cause of change in sediment depth [Plant *et al.*, 1999]. At a range of scales from weeks to years, the migration of sand ridges (also referred to as sand waves or megaripples) contributes to bathymetric variation.

It is a challenge to deterministically model these erosion/accretion patterns which are driven by far-field mechanisms occurring at very much longer time scales (months to years, or even decades) than the elementary processes from which they are built, which occur on time scales of wave events (hours to days) [Hanson *et al.*, 2003]. For the purpose of UnMES, it is required to estimate the probability that the amplitude of bathymetric variation will be comparable to the dimensions of the munitions of concern within some fairly extended time period. To model long-term migration probabilities, the exact temporal phase of short time-scale processes may not be required. For the preliminary UnMES, an empirical approach is taken, with erosion or accretion (E/A) specified statistically, assuming a Gaussian distribution of seabed levels. The input value is given as a standard deviation of vertical variation about the local mean depth (h_{σ}). The choice of the time period over which the variation is determined sets the temporal scale of the model. Similar to the

treatment of d_{sed} , for the GIS implementation a single value ($h_{\text{sigma}} = \text{constant}$) is appropriate within each spatial cell.

Figure 3.8 shows the annual variation of cross-shore bathymetry at FRF, derived from 15 years of survey data [FRF, 2011]. The variation about the mean within each year, is computed, and then averaged over the 15 samples. The standard deviation h_{sigma} is plotted in red over the mean bathymetry in brown. It should be noted that the standard deviation computed over the entire 15 year period is about twice as large as the annual h_{sigma} shown here, so the choice of time scale is an important factor in setting the probability distribution of erosion and accretion.

At two locations, marked by black dots, the histograms of depths are compared with the Gaussian PDFs used to represent them in the E/A node (Figure 3.8b and c). The fits could be improved by including a second parameter quantifying skewness, if the quantity and quality of the bathymetry data warranted the added complexity. The location of the sandbar is characterized by a maximum in h_{sigma} , where changes in seabed level of over 0.35 m occur relatively frequently (about one third of the time). A change of this magnitude is enough to cover or uncover many UXO. Farther offshore, h_{sigma} should approach zero, marking the depth of closure, where the seabed is static over the time scale considered. The standard deviation computed here does not decrease to zero, but asymptotes to about 0.1 m; most likely that is the measurement error for these bathymetric surveys. In Figure 3.8a, the boundaries of spatial cells, based in the water depth discretization, are again indicated by the dashed black lines.

The E/A node is then populated with a normal distribution with mean zero using Netica's internal equation capability. The E/A node must be discretized at intervals fine enough to discriminate changes in percentage burial for the UXO of interest: 5 cm bins are used out to ± 45 cm, then larger intervals (0.5m) to encompass the tails.

A separate node, labeled `ShorelineRetreat` (see Figure 2.1), is included in the BN to capture the process of shoreline erosion and its contribution to UXO unburial, which may be important at some sites. For example, at Camp Perry on Lake Erie, the shoreline retreat has been documented at rates of about 2 m per year, and appears to be a major contributor to the problem of UXO reappearance on the beach [Wilson *et al.*, 2008b]. While this process could be represented using a negative skewness in the E/A distribution, it is clearer to break shoreline retreat out as a separate variable. While the E/A distribution can be developed from data or model results covering a yearly to decadal time scale, the rate of shoreline erosion must usually be estimated by extrapolation of large-scale data sets

[Thieler and Hammar-Klose, 1999], or the use of long-term profile evolution models developed to simulate the response to sea level rise [Hanson *et al.*, 2003]. At some sites, rapid erosion can be triggered by the construction of structures such piers or groins. Estimates from sediment transport models customized to the local beach engineering should provide the mean value to use at each spatial cell in the UnMES GIS.

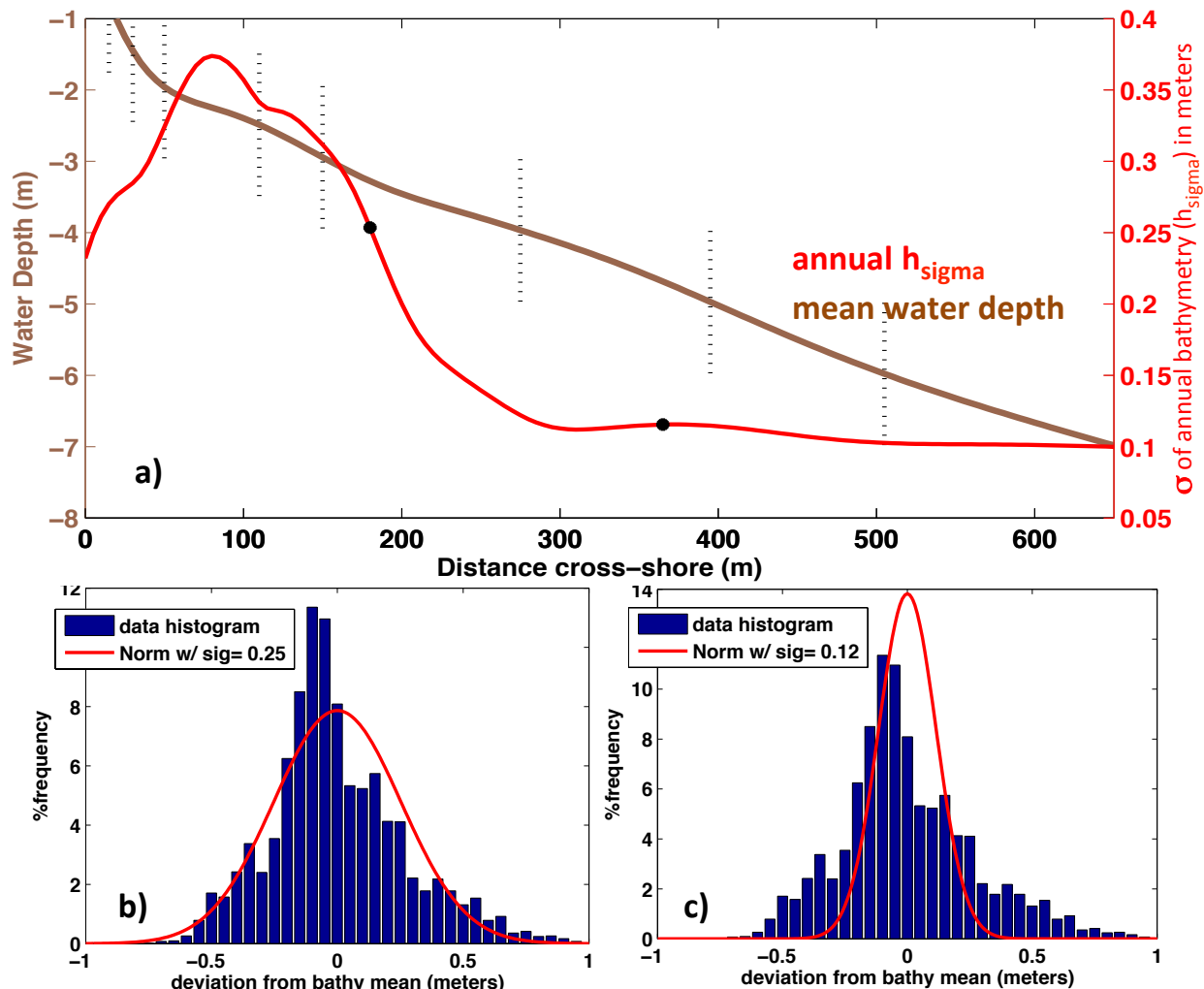


Figure 3.8. Example annual bathymetric variability statistics from a 15 year measurement record at FRF, Duck, NC.

3.6 Intermediate Nodes: Scour Burial and Total Burial

The scour burial node has two parents, U_{bot} and UXO Type (Figure 3.2). The state intervals for the scour burial node were chosen early in the design process (Table 3.1) and have units of percentage, denoting the percent of the UXO diameter that is buried. The CPT for

the scour burial node is built from the equations defining the burial behavior as determined by laboratory and field experiments [Rennie and Brandt, 2014] which is reviewed in Section 4.1 and illustrated in Figure 3.1. Netica allows the specification of a multipart equation; in this initial UnMES, the equation is tripartite with a different parameter used for each of the three example UXO types (Section 3.4.1). When Netica converts an equation to a CPT, a decision must be made as to where within each discretized state to evaluate the equation. Netica's algorithm chooses a number of points at random positions within the state, and uses the average of the results obtained. To reduce sampling uncertainty, the CPTs in UnMES are built using a large number, $O(1000)$, of random points.

Total burial represents the interplay between the predicted scour and impact burial and the erosion or accretion at the cell. The parents for the `TotalBurial` node are `ScourBurial`, `ImpactBurial`, `E/A`, and `UXO Type`, which specifies the UXO diameter. `TotalBurial` is presented in dimensional units (cm) and is discretized to have finer discrimination at low burial (state interval widths of 2, 3, or 5 cm for burial less than 20 cm), but coarser resolution at deeper burial (widths of 10 to 25 cm up to 1 m burial). In this UnMES version, the equation is simply the sum of the dimensional scour burial and `E/A`. Future work will investigate an additional parameter, a multiplicative factor applied to scour burial to adjust for the time scales of the different processes. Figure 3.9 presents an illustration of the section of the BN with `TotalBurial` combining the `ScourBurial` and `E/A` distributions, at a location with the `E/A` parameter set to $h_{\text{sigma}} = 0.12\text{m}$, and zero shoreline retreat. The water depth for the spatial location in this example is $h = 7\text{ m}$, and the `UXO Type` is "bomb", which as a diameter of 15 cm.

3.7 Results Nodes: Migration probability

A number of studies have been conducted to determine the bottom flow required to initiate motion of sediment particles on the seabed. The more relevant literature, involving larger particles (gravel or pebbles) on heterogeneous sediment mixtures, has been extended with laboratory experiments to study the mobility of UXO-sized objects, as described in Section 4.2.

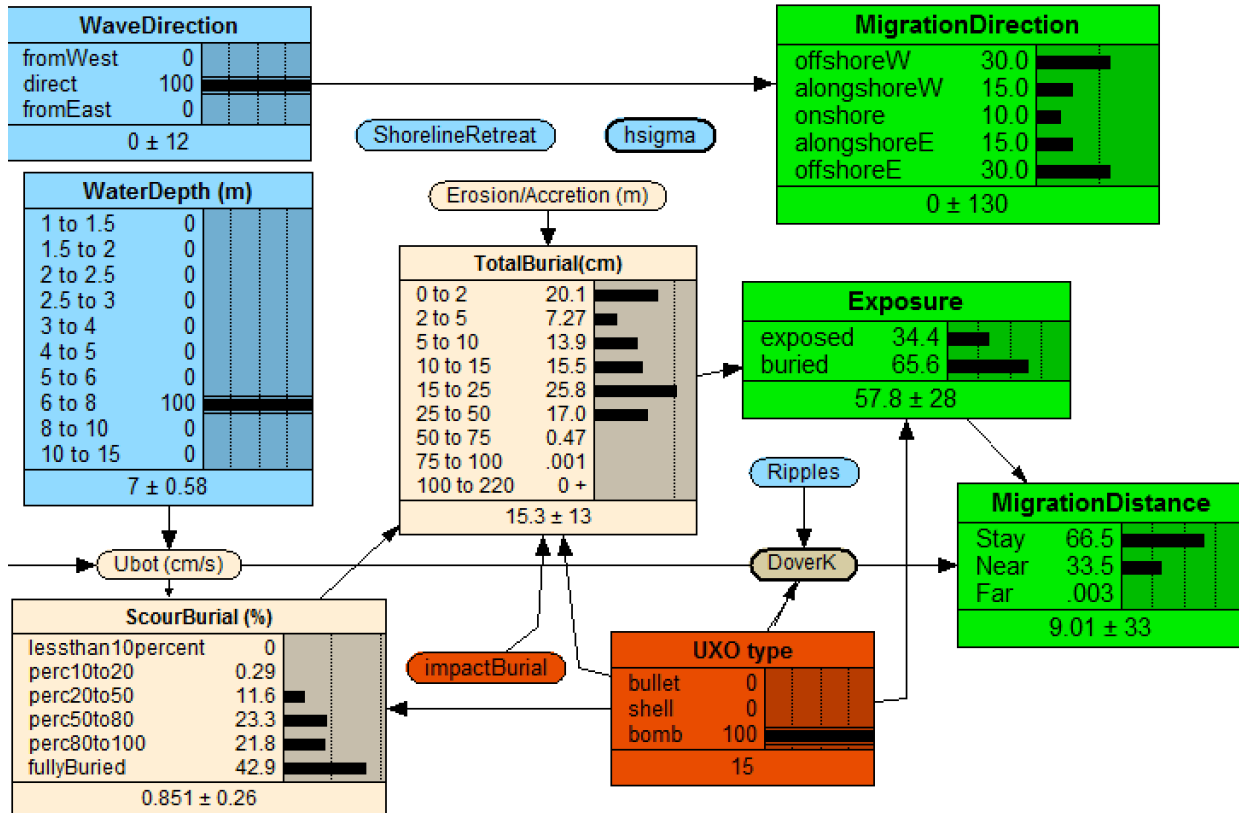


Figure 3.9 Section of the UnMES BN showing Burial and Migration nodes. The wave forcing (not shown) represents a strong event in the location water depth of 7 m.

3.7.1 Migration Distance

In this preliminary UnMES design, the **MigrationDistance** node is partitioned into three states; these are labeled "Stay" for no significant movement; "Near" for distances less than 50 m; and "Far" for further movement. An intermediate node called **Exposure** is introduced to determine whether the UXO is "locked down" by burial. The **Exposure** node has two states: "exposed" when **TotalBurial** is less than half the UXO diameter, and "buried" for all other conditions. The CPT entries in the **MigrationDistance** node with the parent state "buried" are all set to "Stay". If "exposed", then the probability of motion is based on the bottom velocity distribution and UXO density (formulated as the Object Shields parameter discussed in Section 4.2) compared to the UXO size versus the bottom roughness scale, represented by the node **DoverK**.

While the equation to compute a threshold of mobilization is given in Section 4.2, there is little guidance yet on how far the UXO will travel once motion is initiated. For the current

UnMES implementation, an *ad hoc* formulation is utilized. When the mobility threshold is just slightly exceeded (i.e. Object Shields parameter within an order of magnitude of the threshold) UXO are envisioned to slide or roll along the seabed. Laboratory studies of rolling cylinders [Davis *et al.*, 2007] show the object velocity to be about 70% of the bottom flow speed. Therefore, for these cases a rule-of-thumb distance is estimated based on the speed $0.7 \cdot U_{\text{bot}}$, acting over half the wave period. When the forcing strongly exceeds the mobility threshold (by more than one order of magnitude), the object travels suspended in the current, and a full 100% of U_{bot} is used. When the forcing dramatically exceeds the threshold (more than two orders of magnitude), it is assumed that conditions are such that the entire seabed is mobilized, with burial unlikely, and multiple instances of mobilization occur. Only these extreme conditions can generate migration in the “Far” state. These *ad hoc* rules make the `MigrationDistance` node conditionally dependent on at least five parent nodes. To refine these coarsely-determined migration estimates will require further research, especially the inclusion of results from recent field experiments in energetic conditions.

3.7.2 Migration Direction

Because generally detailed knowledge is lacking about the direction that a UXO will move, the `MigrationDirection` node is discretized into a small number of states. `MigrationDirection` is set up representing directional quadrants: onshore ($\pm 45^\circ$), “east” (to the left facing onshore), “west”, and offshore (which is separated into two states to encompass -180 to -135° and $+135$ to $+180^\circ$). A straightforward prediction of migration direction, proceeding from a simple assumption of mobilization during the passage of a wave’s crest, will be onshore, with some component of alongshore, based on the input wave direction. However, consideration of the general tendency of objects to migration downslope increases the likelihood of offshore movement. A detailed CFD modeling study using the UXO-MM code [Jenkins *et al.*, 2013] at a site Adak, AK, driven by a 20-year wave record, showed that the dominant direction of movement was offshore, with less than 10% of the modeled migration towards the beach, and about a third traveling alongshore. Field studies over 3 to 5 months offshore of FRF at Duck, NC [Wilson *et al.*, 2008a] reported onshore movement for 12% to 20% of the UXO surrogates, with offshore migration in a third to a half of the observations. Our ability to predict the dominant direction of UXO migration will require additional site-specific environmental knowledge, such as prevalence of the longshore current. For the current UnMES implementation, a prior PMF is assigned to the `MigrationDirection` node that reflects the long-term Adak model results, and is shown in Figure 3.9.

4 Core Physics: process models in UnMES

Process models for UXO scour burial, mobility and re-exposure are at the core of the UnMES. Significant progress has been made on development of appropriate models for UXO burial and mobility based on the extant literature, available field data and experiments designed specifically for the properties of UXO (size and density). A brief summary of these models is presented below while the details of their development are presented in Rennie and Brandt [2014]. Appropriate process models for UXO re-exposure are currently under development.

4.1 Scour Burial Model

Water flow, either the oscillatory motion of waves, or steady currents, is accelerated in the vicinity of an object lying on the seabed, causing sediments to erode at the ends of the UXO. Scour pits are thus formed, and, as scouring continues, the UXO falls into the enlarging pit. The pit then becomes a sediment trap and can fill in. This process and the following process model results are described in Rennie and Brandt [2014].

As the extant data on scour around finite objects is quite limited. Available studies include a laboratory study by Demir and García [2007] on cylinders in oscillatory flow, field studies of large sea-mine surrogates [Trembanis et al, 2007]. and a series of experiments utilizing UXO surrogate shapes conducted at JHU/APL [Rennie and Brandt, 2014]. In these recent studies large “shell” like cylinders, tapered cylinders and small “bullet” sized cylinders were utilized.

The results and prior data are shown in Figure 4.1, where the fraction of final scour burial is plotted as a function of the sediment Shields parameter, θ , which is the dimensionless parameter that encompasses the driving parameter for the scour process. θ is defined as

$$\theta = \frac{\frac{1}{2}f_\tau U^2}{g (S_{sed}-1)d_{sed}}, \quad (4.1)$$

where U the bottom current, g gravitational acceleration, $S_{sed} = \rho_s/\rho_w$, with ρ_s the sediment grain density, ρ_w the water density, and d_{sed} the median sand grain size. The friction drag force coefficient f_τ represents the skin-friction shear stress acting on the bed, rather than the form drag acting on any individual sand particle (Soulsby, 1997).

Figure 4.1 shows the previously compiled laboratory data [Demir and García, 2007], labeled “DG2007” and field data [Trembanis *et al.*, 2007], labeled “ONR MBP FIELD.” Red circles indicate JHU/APL laboratory results using cylinder with diameter $D = 10$ cm. Brown triangles show the burial observed with the tapered cylinder ($D = 7.94$ cm). The small diameter ($D = 2.54$ cm) cylinders shown as magenta circles. The considerable scatter apparent is the result of the natural variability of the turbulent scouring process, the variability in the scour pit growth and differences in the local sediment environment.

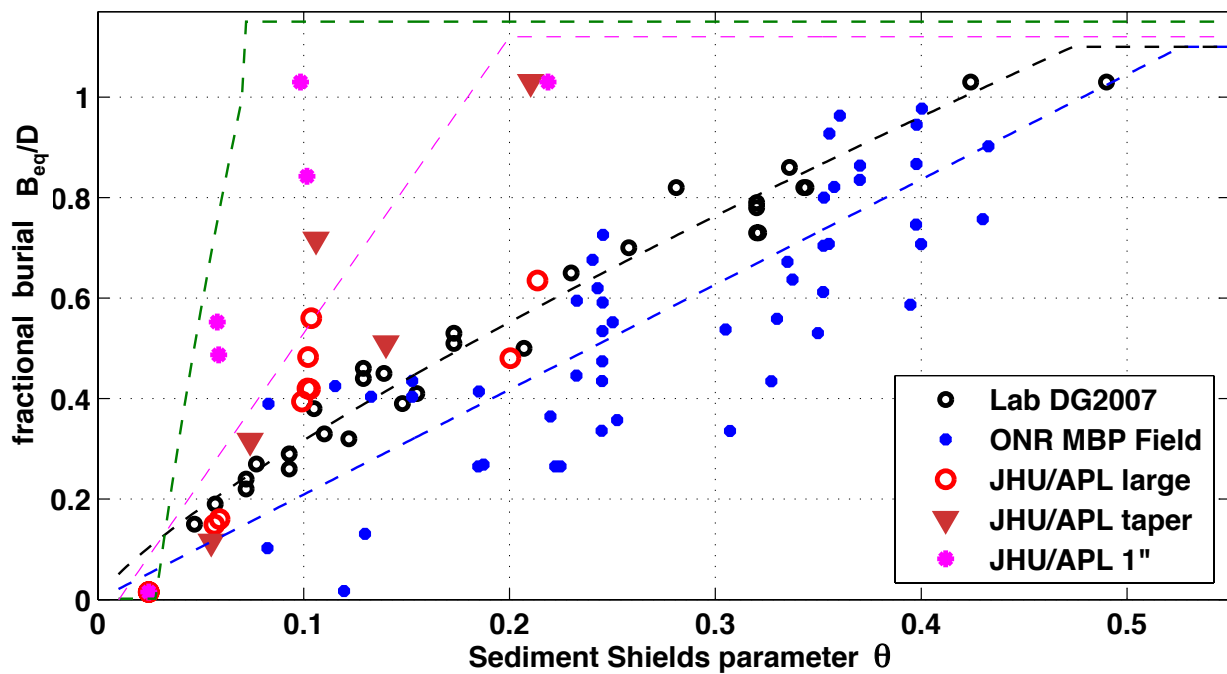


Figure 4.1. Observations of scour burial of UXO and sea-mine surrogates. Burial is reported as the fraction of the surrogate diameter and plotted versus the Sediment Shields number θ .

It was found that the burial fraction can be reasonably represented by the relationship

$$\frac{B_{eq}}{D} = a \theta^b, \quad (4.2)$$

where B_{eq} is the equilibrium burial depth and a and b are empirically determined constants. This relationship gives a reasonably simple process model for burial depth for use in the UnMES that relates the UXO properties to the environmental conditions through the Shields parameter.

The blue, black and green dashed lines show the empirical fits to Equation 4.2 from Friedrichs [2014], Demir and García [2007] and Whitehouse [1998], respectively. For large, cylindrical objects, b lies between 0.8 and 1.0 and a is about 2.2. The scale factor a is larger for tapered shapes or very small UXO such as bullets, which exhibited a tendency to bury more easily. The magenta line represents the best fit of Equation 4.2 for the combined tapered and small UXO observations with values of $a = 5.9$ and $b = 1$. These empirical parameters are applied in the Netica equations defining the CPT for the ScourBurial node (Section 3).

4.2 Mobility Model

Motion of a bottom-sitting object results when the force on the object due to its drag in the local flow exceeds the resisting force due to the objects weight and inertia. For large objects compared to the bed sand grain size, the appropriate parameter governing the criteria for the onset motion is the Object Shields number θ_{obj} [Friedrichs, 2015] defined in analogy to the Shields parameter, θ , as

$$\theta_{obj} = \frac{U^2}{g (S_{obj} - 1) D} , \quad (4.3)$$

where the object diameter, D , replaces the characteristic sand grain size, d_{sed} , and the specific gravity of the object, S_{obj} , replaces the specific gravity of the sand grains used in Equation 4.1.

Figure 4.2 shows the mobility threshold, θ_{obj} , data plotted versus the ratio of the object diameter D to bed roughness, k . This ratio D/k , parameterizes geometrical aspects of the force balance, and is represented by the BN node `DoOverK` in UnMES. The prior extant data considered large objects in field studies shown in green, magenta and brown on the right and the motion of the particles from a it sand bed itself in black on the left (see Rennie and Brandt [2014] for details). As UXO fall in the intermediate range that was not covered, a series of laboratory studies were performed to provide these data, shown as red symbols.

The solid blue in Figure 4.2 line is the best fit power law for all data, while the red line shows the fit for $D/k > 4$ excluding field data of natural sediments, with dashed lines indicating the 95% confidence limit. This latter curve provides the process model needed in UnMES as

$$\theta_{\text{obj}} = 1.2 (D/k)^{-0.62} \quad (4.4)$$

Equation 4.4 is used in the definition the CPT of the MigrationDistance node (Section 3.7). It should be noted that the onset of UXO motion for objects on a sand bed is somewhat more complicated due to the fact that some scour may occur prior to the onset of motion which will alter the flow pattern around the UXO and thus the appropriate value of θ_{obj} , as discussed in Rennie and Brandt [2014].

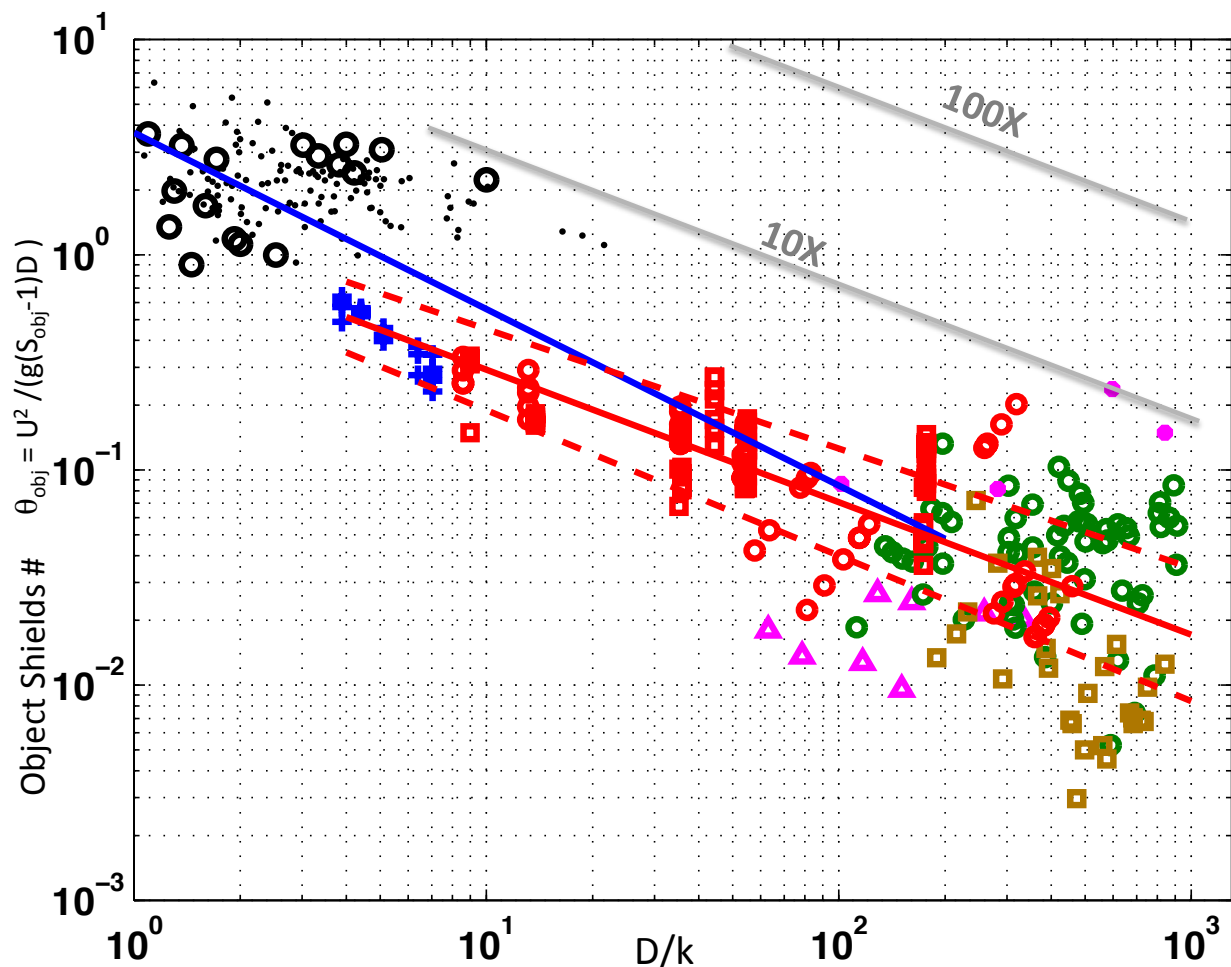


Figure 4.2. Compiled data for the mobility threshold of objects on the seabed. JHU/APL laboratory results shown are in red. The solid blue line is the best fit power law for all previous and new data combined; the red line shows the fit for $D/k > 4$, which excludes field data of near-homogenous sediments. The dashed lines indicate the 95% confidence limit around the large D/k fit. The grey lines indicate the state interval boundaries for the Object Shields parameter, delimiting different defined modes of migration behavior (Section 3.7.1).

4.3 Re-exposure Models

Predicting the probability of re-exposure is a particularly important factor in estimating migration potential, as UXO can be mobilized only when buried less than about half of its casing diameter. In addition, estimation of the percentage of time spent covered by sediment is important to predicting the condition of the munitions' casings. Complete burial in anoxic conditions can result in casings displaying very little corrosion even after decades, whereas prolonged periods of exposure on the seabed results in corroded, leaking UXO. Prediction of the casings' condition could be included in future versions of UnMES that tackle the problem of estimating seawater pollution from dissolved chemical components of munitions.

Re-exposure is the result of temporal changes in far-field sediment morphology with different processes dominant at different time-scales. At the MR Program Review Workshop [SERDP, 2014], it was noted that progress is needed in modeling far-field processes in order to understand long-term UXO migration patterns. The proposed continuation of the present study [Rennie and Brandt 2015a], in collaboration with the upcoming SERDP Project MR01-026 [Friedrichs, 2015] will develop improved parameterized model formulations describing far-field phenomenology including ripple and dune migration as well as larger-scale shoreward movement of the shoreline and associated shoreface, both cyclical (e.g., winter/summer beach profile adjustments) or unidirectional (e.g., net coastal erosion). The current version of UnMES uses a data-derived statistical representation of exposure probability (Section 3.5) as a placeholder until these far-field process models are sufficiently developed.

5 Example Implementation

Environmental data is being gathered in order to populate the input GIS layers for two example implementations of UnMES: the Gulf of Mexico (GoM) off the coast of Panama City (shown in Figures 3.3 and 3.4); and at the FRF in Duck NC (Figures 3.5 and 3.6). These sites are chosen because field test observations will be available for future comparison with UnMES predictions for verification of the expert system utility. The behavior of a number of surrogate munitions deployed in the GoM was studied during the TREX13 field test [Calantoni, 2015] in April through May 2013. An earlier field test was conducted at FRF over a more extended period of time in 2005 to 2006 [Wilson *et al.*, 2008a].

In Figures 3.2 and 3.9 sections of the UnMES core BN are shown for the GoM example. Figure 3.2 illustrates the Scour Burial response for a wave height distribution representative of the coast off Panama City in shallow water (h is between 2.5 and 3 m). The characteristics of each node are displayed as “belief bars”, the probability distribution approximated by a PMF (normalized histogram). At this water depth, which is inshore of the sandbar dissipation has reduced all larger offshore waves so that $H_{sig} < 1.4$ m, resulting in a local peak in the wave height distribution in the state “1.2 to 1.4 m”. The wave period distribution is based on observations, so that its relationship with wave height is represented. Here the mean period is 5.9 ± 2.7 s, which is displayed at the bottom of the Period node. The distribution of bottom orbital velocity is computed by Netica in the U_{bot} node using the linear wave equations. The UXO Type input node is set to all of state “shell” (Section 3.4.1). The seabed sediment is composed of medium sand grain size $d_{sed} = 0.45$ mm, so that scour process falls in between that of very fine and coarse sand behavior as shown in Figure 3.1. Note that because d_{sed} is treated as a Netica constant, that node’s value is available to all other nodes in the BN without a link (arrow).

Because the Wave Height node here represents the distribution of wave conditions over an extended temporal period, the ScourBurial PMF can be interpreted as the percentage of time for which conditions are such that a proud UXO would become buried. The ScourBurial node computes a $\sim 27\%$ chance of very slight burial (less than 10% buried) that corresponds approximately to the combined probability of the two lowest states in the U_{bot} distribution, representing bottom flow speeds less than 20 cm/s, and consistent with Figure 3.1. Note that state intervals for a node may have different widths – this can result in a PMF’s belief bars appearing oddly irregular. For example, the first two ScourBurial states encompass 10 percentiles, while the central two states are wider, and therefore contain a larger portion of the PDF, even though the probability of degree of burial is actually decreasing monotonically. The state “fully buried” is populated with all possibilities where wave forcing is strong enough to arrive at equilibrium burial, which is quantified as a burial depth of 115% the object diameter [Whitehouse, 1998]. Given the empirically-determined parameters for the burial behavior of a “shell” type UXO (Section 4.1), the “fully buried” state occurs for all $U_{bot} > 60$ cm/s, and therefore contains the sum of the probabilities over the six highest U_{bot} states.

The section of the UnMES BN addressing Total Burial and Migration is shown in Figure 3.9. In this example the wave conditions represent a storm event ($H_{sig} \sim 2.5$ m, WaveHeight node not shown), in a water depth of ~ 7 m. The UXO Type modeled is “bomb” which is larger and less dense than the other types. Initial impact makes no contribution to burial in

this example. After storm conditions, the `ScourBurial` node reports the large majority (88%) of the bomb casings would likely be more than half buried. However, the possibility of seabed erosion at the site reduces that likelihood somewhat, so that “buried” state in the `Exposure` node is less than 66%. Of the exposed UXO, most are predicted to remain in their original positions (“Stay” is the most probable state in `MigrationDistance`), while about one third are predicted to move a short distance. There is an almost zero probability predicted for substantial “Far” migration. A comparison of UnMES predictions with field observations is currently in progress and will be reported in the forthcoming Demonstration Report on the prototype UnMES implementation [Rennie and Brandt, 2015b].

6 Summary and Future Work

The preliminary design for the Underwater Munitions Expert System (UnMES) is described. UnMES is a computer-based probabilistic expert system to predict the likelihood of burial and migration of abandoned underwater munitions. This approach utilizes simple deterministic models in a probabilistic framework, combined with statistical parameterizations to define the joint conditional probability space for UXO behavior. Probabilistic modeling is appropriate given the inherent uncertainties in a munitions site’s history and imperfect knowledge of the environment and complex physical processes governing UXO burial and mobility. UnMES will be a component of a larger risk assessment tool developed for use by site managers as remediation guidance. This larger framework will require GIS support for environmental input and visualization of spatially varying assessments. The Bayesian network for the prototype UnMES makes use of the GeoNetica software product, and a QGIS framework to interpret and display map-based information.

The component variables of the Bayesian network are specified as belonging to input, output, and intermediate node sets. The interrelationships between nodes determines the causal structure of the predictive system. Methods are developed to determine the required discretization of the continuous variables delimiting the states of each node, balancing the need for adequate resolution with operational tractability. Future work will investigate the application of alternative probabilistic programming environments which can handle continuous distributions with techniques for performing the Bayesian inference parametrically. This would eliminate the requirement to make prior selections of the state intervals for discretizing the PDFs.

Environmental data from two sites of interest are compiled in QGIS layers and are being used as input to the prototype UnMES implementation. The task of demonstration and

verification of UnMES predictions is being undertaken using field test observations from recent SERDP-funded experiments conducted in wave-dominated coastal locations off Florida and North Carolina. Additional environmental data will be acquired from the field experiments near Martha's Vineyard [Traykovski, 2015]. Access to details of these UXO burial and migration observations should be available in the near future.

The Underwater Munitions Expert System will be part of a decision support tool providing graphical mapping and visualization of UXO distributions and burial state for site remediation planning. A key aspect of the continued development of UnMES will be forming the metrics by which prediction uncertainty can be presented and assessed for the evaluation of management alternatives. A QGIS plug-in, the Probabilistic Map Algebra Tool (PMAT) [Landuyt *et al.*, 2015], is under evaluation for possible use. PMAT produces different formats of Bayesian belief network maps to aid in understanding risk, including (1) the most probable state accompanied by a map of the probability of that reported state; and (2) a map of expected value along with a second map of standard deviation cumulative probability below or above a specified threshold. These formats will be evaluated during the prototype UnMES evaluation.

Use of the preliminary UnMES design has made clear that additional work needed on understanding re-exposure probabilities. Further research is proposed [Rennie and Brandt, 2015b, Friedrichs, 2015], to develop rational parameterized models for UXO re-exposure due to far field effects such as seasonal beach profile shaping as well as sand wave or large bedform migration. Other topics requiring additional research are the potential for impact burial and a better understanding of the distance that munitions can travel once mobilized.

Literature Cited

- Calantoni, J. 2015 "Long Time Series Measurements of Munitions Mobility in the Wave-Current Boundary Layer," SERDP Project MR-2320, In-Progress Review.
- Chu, P.C., Bushnell, J.M., Fan, C., Watson, K.P. 2011 Modeling of Underwater Bomb Trajectory for Mine Clearance, *J. Defense Modeling and Simulation*, 8(1), 25-36.
- Davis, J. E., Edge, B. L., & Chen, H. C. 2007. Investigation of unrestrained cylinders rolling in steady uniform flows. *Ocean engineering*, 34(10), 1431-1448.
- Demir, S.T., García M.H. 2007 Experimental Studies on Burial of Finite Length cylinders under Oscillatory Flow, *J. Waterway, Port, Coast, and Ocean Eng.*, ASCE, 133 (2), 117-124.
- Friedrichs, C.T. 2015 "Parameterized Process Models for Underwater Munitions Expert System," Proposal to SERDP BAA-15-0001, MRSN-16-01, SERDP Munitions Response (MR) Program Area, Virginia Institute of Marine Science.
- FRF 2011 Field Research Facility, Field Data Collections and Analysis Branch, US Army Corps of Engineers, Duck, North Carolina. <http://frf.usace.army.mil>,
- Guenther, G.C., Cunningham, A.G., LaRocque, P.E., Reid, D.J. 2000 Meeting the accuracy challenge in airborne lidar bathymetry, *Proc. 20th EARSeL Symposium: Workshop on Lidar Remote Sensing of Land and Sea*, June 16-17, Dresden, Germany, European Association of Remote Sensing Laboratories, 23 pp.
- Gutierrez, B.T., Plant, N.G., Thieler, E.R. 2011 A Bayesian network to predict coastal vulnerability to sea level rise, *J. Geophys. Res.*, 116.F2.
- Holland, K.T. 2014 A "Wide Area Risk Assessment Framework for Underwater Military Munitions Response," *Workshop on Burial and Mobility Modeling of Munitions in the Underwater Environment*, Strategic Environmental Research and Development Program, Arlington, VA, June 30, 2014.
- Hanson, H., Aarninkhof, S., Copabianco, M., Jimenez, J.A., Larson, M., Nicholls, R.J., Plant, N.G., Southgate, H.N., Steetzel, H.J., Stive, M.J.F., de Vriend, H.J., 2003 Modelling of coastal evolution on yearly to decadal time scales, *J. Coastal Res.* 19 (4), 790-811.
- Holman, R. A., Stanley, J. 2007 The history and technical capabilities of Argus, *Coastal Engineering*, 54, 477-491.
- Jenkins, S.A. Inman, D.L. 2006 Thermodynamic solutions for equilibrium beach profiles, *J. Geophys. Res.*, 111, 1-21.
- Jenkins, S., D'Spain, G., Wasyl, J. 2012, "Vortex Lattice UXO Mobility Model for Reef-Type Range Environments," ESTCP Project MR-201003, Final Report.
- Jenkins, S., D'Spain, G. Wasyl, J. 2013, "Hydrodynamic Mobility Analysis of UXO Transport, Andrew Bay Adak Island, Alaska," Scripps MPL Report to Munitions Response, Battelle, 99 pp.

- Jensen, F.V., Nielsen, T.D. 2007, Bayesian Networks and Decision Graphs, Springer, New York.
- Koller, D., Friedman, N. 2009 Probabilistic Graphical Models: Principles and Techniques, MIT Press, Cambridge, MA.
- Landuyt, D., Van der Biest, K., Broekx, S., Staes, J., Meire, P., Goethals, P.L.M. 2015 A GIS plug-in for Bayesian belief networks: Towards a transparent software framework to assess and visualize uncertainties in ecosystem service mapping," *Env. Modelling & Software*, 71, 30-38.
- Laskey, K. B., Wright, E. J., da Costa, P C.G. 2010 Envisioning uncertainty in geospatial information," *Internat. J. Approximate Reasoning*, 51, 209-223.
- MATLAB version R2014B 2014 The MathWorks Inc., Natick, Massachusetts.
- Norsys, 1995–2015 Netica™ of Norsys Software Corp., Ver. 5.15, www.norsys.com.
- Pearl, J. 1991 Probabilistic Reasoning in Intelligent Systems: Networks of Plausible Inference, 2nd ed., Morgan Kaufmann, San Mateo, CA.
- Plant, N. G., Holland, K.T. 2011 Prediction and assimilation of surf-zone processes using a Bayesian network. Part I: Forward models, *Coastal Eng.*, 58 (1), 119-130.
- Plant, N. G., Holman, R.A., Freilich, M.H., Birkemeier, W.A. 1999 A simple model of interannual sandbar behavior, *J. Geophy. Res.* 104 (C7), 15755-15776.
- QGIS, 2015. Open Source Geospatial Foundation (OSGeo), www.qgis.org.
- Rennie, S. E., Brandt, A., Plant, N. 2007 A Probabilistic Expert System Approach for Sea Mine Burial Prediction, *IEEE J. of Oceanic Eng.*, 32 (1), 260-272.
- Rennie, S.E., Brandt, A. 2014 "Experimental Determination of Underwater Munitions Mobility and Burial," Johns Hopkins Univ. Applied Physics Laboratory, Technical Memorandum, FPS-T-14-0575, December 2014.
- Rennie, S.E., Brandt, A. 2015a "Underwater Munitions Expert System for Remediation Guidance," Proposal to SERDP BAA-15-0001, MRSON-16-01, SERDP Munitions Response (MR) Program Area, Johns Hopkins Univ. Applied Physics Laboratory, March 2015.
- Rennie, S.E., Brandt, A. 2015b "Demonstration Report of a Prototype Underwater Munitions Expert System," Johns Hopkins Univ. Applied Physics Laboratory Technical Memorandum, *in preparation*.
- Ruggiero, P., List, J., Hanes, D., Eshleman, J. 2006 "Probabilistic Shoreline Change Modeling," 30th Interna. Conf. Coastal Engineering, San Diego, CA.
- SERDP 2014 "Informal Workshop on Burial and Mobility Modeling of Munitions in the Underwater Environment," Strategic Environmental Research and Development Program, Final Report, V.2.0, 31 Dec., 2014, 22 pp.
- Settelmaier, J. B., Gibbs, A., Santos, P., Freeman, T., Gaer D., 2011 "Simulating Waves Nearshore (SWAN) Modeling Efforts at the National Weather Service (NWS) Southern Region (SR) Coastal Weather Forecast Offices (WFOs)," *Proc. 91st AMS Ann. Mtg.*, Am. Meteor. Soc., Seattle, WA.

- Smith, J.M., Resio, D.T., Zundel, A.K. 1999 "STWAVE: Steady-state spectral wave model," Instruction Report CHL-99-March 1999, U.S. Army Engineering Waterways Experiment Station, Vicksburg, MS.
- Soulsby, R. 1997 Dynamics of Marine Sands, HR Wallingford, Thomas Telford, London.
- Thieler, E. R., Hammar-Klose E.S. 1999 "National assessment of coastal vulnerability to future sea-level rise, Preliminary results for U.S. Atlantic Coast," U.S. Geol. Survey, Open File Rep., 99-593.
- Thornton, E.B., Guza, R.T. 1983 Transformation of wave height distribution. *J. Geophys. Res.* 88 (C10) 5925–5938.
- Tolman, H.,L. 2009 "User manual and system documentation of WAVEWATCH III™," version 3.14,. NOAA/NWS/NCEP/MMAB Tech. Note 276, 194 pp + Appendices.
- Traykovski, P. 2015 "Continuous Monitoring of Mobility, Burial, and Re-Exposure of Underwater Munitions in Energetic Near-Shore Environments," SERDP Project MR-2319, In-Progress Review.
- Trembanis, A., C. Friedrichs, M. Richardson, P. Howd, P. Traykovski, P. Elmore, and T. Wever, 2007. "Predicting Seabed Burial of Cylinders by Scour: Application to the Sandy Inner Shelf off Florida and Massachusetts", *IEEE J. Ocean. Eng.*, vol. 32, no. 1, pp. 167–183.
- USEPA 2007 "Better Assessment Science Integrating Point and Nonpoint Sources – BASINS" version 4.0, EPA-823-C-07-001. Washington, D.C, U.S. EPA, Office of Water. Available at: www.epa.gov/waterscience/basins/.
- van der Westhuysen, A. J. 2012 "Modeling nearshore wave processes," ECMWF Workshop on Ocean Waves, June 2012.
- Wells, D. E., & Monahan, D. 2002. IHO S44 standards for hydrographic surveys and the variety of requirements for bathymetric data. *Hydrographic Journal*, 9-16.
- Whitehouse, R. 1998 Scour at Marine Structures, HR Wallingford, Thomas Telford, London.
- Wilson, J. V., McKissick, I., Jenkins, S. A., Wasyl J., DeVisser A., Sugiyama, B. 2008a "Predicting the Mobility and Burial of Underwater Munitions and Explosives of Concern Using the VORTEX Model," Final Report, ESTCP Project MM-0417.
- Wilson, J. V., DeVisser A., Sugiyama, B. 2008b "Example Application Analysis (Lake Erie Impact Range)," ESTCP Project 200417, September 2008.